

UNIVERSITY OF MASSACHUSETTES AT LOWELL
RESEARCH REACTOR
LICENSE NO. R-125
DOCKET NO. 50-223

POWER UPRATE APPLICATION
FINAL SAFETY ANALYSIS REPORT (FSAR)
SUPPLEMENT

REDACTED VERSION*

SECURITY-RELATED INFORMATION REMOVED

*REDACTED TEXT AND FIGURES BLACKED OUT OR DENOTED BY BRACKETS

**FSAR SUPPLEMENT FOR POWER UPGRADE FROM
1 MW to 2 MW STEADY STATE POWER**

FOR

**THE UNIVERSITY OF MASSACHUSETTS LOWELL (UML)
RESEARCH REACTOR**

**Prepared by UML Staff
with assistance of**

**Research Reactor Safety Analysis Services
Kennewick, WA**

July 7, 2006

EXECUTIVE SUMMARY

This report presents a description and safety evaluation of the University of Massachusetts Lowell Reactor (UMLRR) for an increase in steady-state power rating from 1 MW to 2 MW thermal under License R-125.

The UMLRR is a light-water, moderated and cooled, graphite-reflected, heterogeneous, open-pool type research reactor. The reactor was designed, manufactured, and installed by the General Electric Company. For conservative measure, the reactor was initially licensed for 1 MW in 1974 and similarly re-licensed in 1985. However, the original design rating of the reactor and its cooling systems was 2.5MW_t , while the containment building, pool structure, and coolant piping were designed and built for 5MW_t operation. The UMLRR remains one of only three USNRC licensed research reactors in the U.S. with a full containment building.

The general description of the facility is unchanged from the current FSAR in terms of history of the facility, location, general housing, reactor building, and backup systems. In 1993, a supplement to the FSAR was submitted to the NRC in support of conversion from HEU to LEU fuel. The reactor was converted from HEU to LEU fuel in 2000. Changes to the reactor core and in some related systems have occurred since the 1993 supplement and are presented in the report.

For this supplement, the thermal hydraulic computer codes NATCON, PLTEMP, and PARET-ANL have been used to determine the limiting conditions for safe operation of the current UMLRR LEU core at 2 MW under steady-state natural-convection, steady-state forced-convection, and transient conditions, respectively. These codes allow the user to set values for the power, flow rate, and in the case of PARET-ANL, reactivity transients, to determine what combinations of these parameters cause the onset of nucleate boiling (ONB) to occur. The ONB point is used as the conservative criterion for determining the safe operating conditions of the UMLRR.

The NATCON steady-state convection thermal hydraulic computer code was used to determine the ONB point under natural-convection flow conditions. Hot channel factors were incorporated in the model to represent uncertainties in the flow rate, power level, and heat transfer coefficient. The ONB point was determined to occur at a power level of 392 kW with a natural convection flow rate of 126 gpm.

The PLTEMP steady-state forced-convection thermal hydraulic computer code was used to create two power-to-flow curves – one with and one without hot channel factors. The results of the power-to-flow curves are used to define the steady-state operating envelope for the UMLRR and to bench mark the differential between calculations done with 100% certainty and those using hot channel factors. The margin between the two curves varied from approximately 60% at low power levels to approximately 75% at high power levels. For a power level of 2 MW using hot channel factors, ONB was found to occur between a flow rate of 702 to 707 gpm during steady-state conditions. These results are shown in Figure 1.

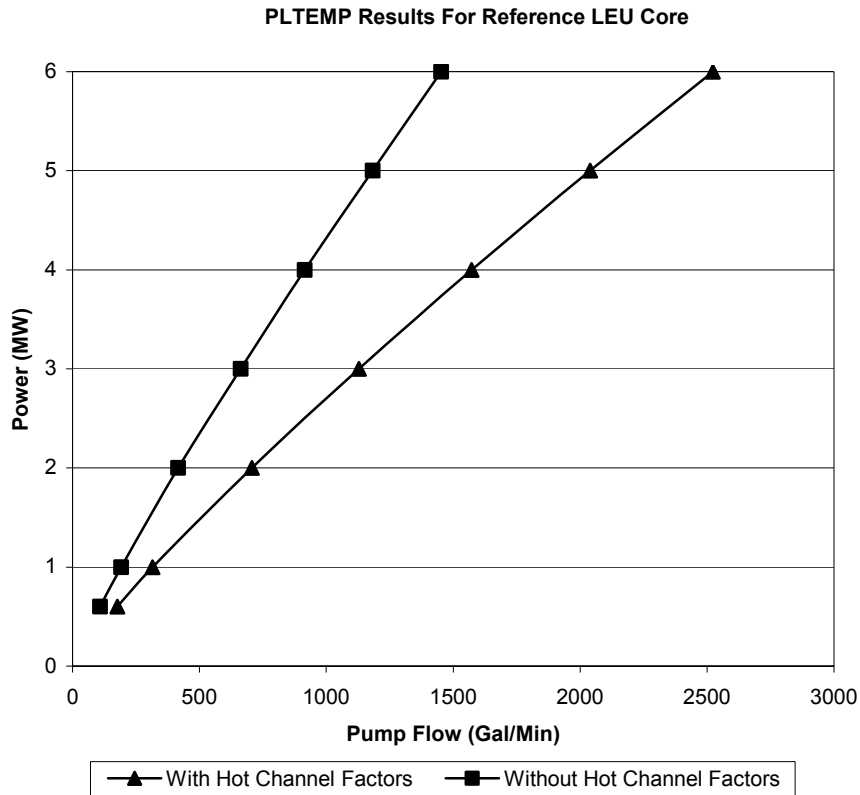


FIG. 1: PLTEMP POWER-TO-FLOW MAP

To address transient conditions, the PARET-ANL transient thermal hydraulic computer code was used to determine the limiting conditions of operation for various reactivity transient and loss-of-flow scenarios. It was determined that the most limiting case was for an instantaneous, or step-change reactivity excursion of 0.5% $\Delta k/k$ (64 cents). This corresponds to a single-failure criterion of one fixed sample of maximum reactivity-worth instantaneously ejecting from the reactor core. From this base case, the limiting conditions of power and flow to prevent ONB from occurring during the transient were determined. The analyses were done for several power levels ranging from 100 kW to 6 MW. At a power level of 2 MW, ONB was found to occur between a flow rate of 505 and 510 gpm during the worst-case reactivity transient.

However, unlike PLTEMP, the PARET-ANL code does not have the capacity to model hot channel factors. To simulate the effects of this, a 75% margin reflecting the highest deviation in the corresponding PLTEMP curves was graphed along with the normal PARET-ANL ONB curve. This is shown in Figure 2. This margin represents the best estimate of the combination of all hot channel factors as a worst-case scenario uncertainty. A similar natural convection low power-low flow region is shown in Figure 3. The power-to-flow map was expanded into two plots to highlight the two proposed nominal operating regimes for the UMLRR, i.e. natural-convection mode at low power (200 kW) and forced-convection mode at high power (2 MW). These plots show that, even with large uncertainties included, transient ONB will not occur with a 0.5% $\Delta k/k$

step-reactivity change during either natural- or forced-convection operation. The transient ONB curve is proposed as the safety criterion for any operational transients to prevent ONB from occurring in the UMLRR LEU core.

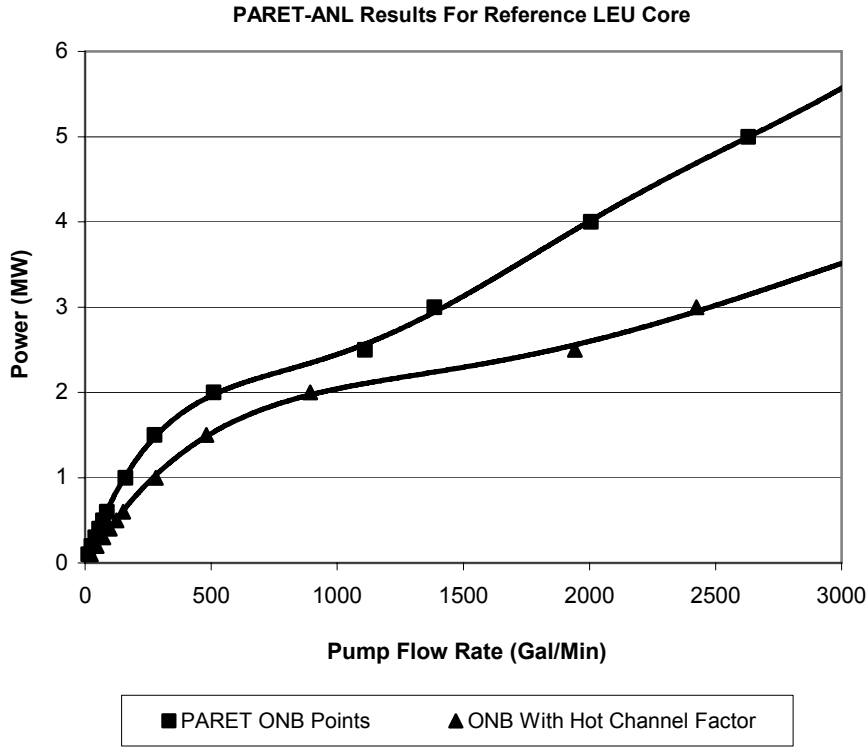


FIG. 2: PARET-ANL HOT CHANNEL POWER-TO-FLOW MAP

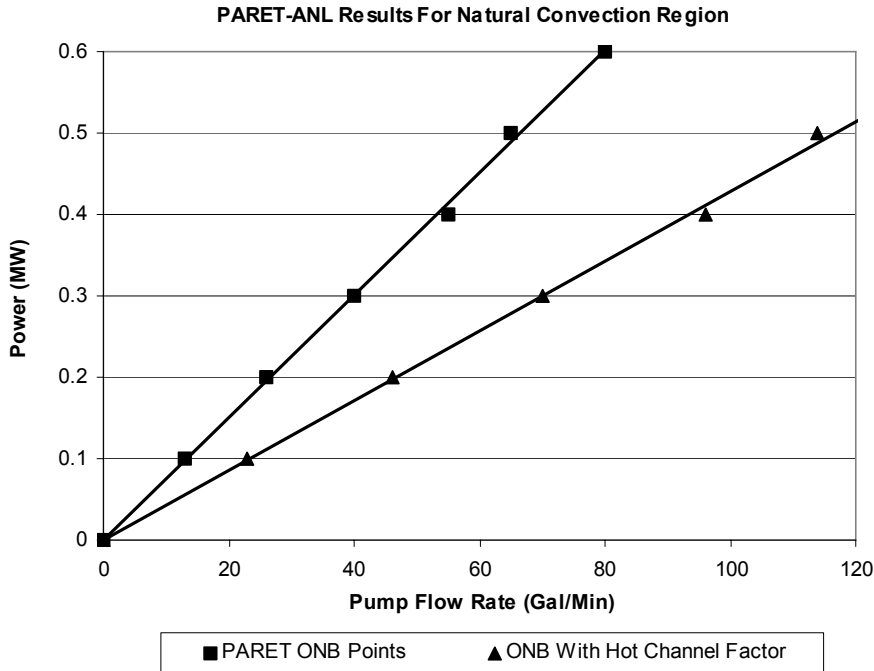


FIG. 3: PARET-ANL NATURAL CONVECTION POWER-TO-FLOW MAP

As a final comparison, a plot of the steady-state and transient power-to-flow ONB curves, including the effects of hot channel factors, is shown in Figure 4. As expected, the transient case for a 0.5% $\Delta k/k$ step-reactivity change reduces the safe operating region of the power-to-flow map relative to the steady-state case. The lower curve, which represents the transient ONB hot channel factor power-to-flow map, gives the best estimate of when ONB would occur, using conservative hot channel factors, for all foreseen accident conditions. The use of the transient ONB condition was shown to give a conservative safety margin for the worst-case reactivity transient under both forced-flow and natural-convection conditions. Thus, the transient ONB results given here can be used to set the actual safe operating limits for the UMLRR. In particular, it shows the UMLRR can be operated safely at 200 kW in natural-convection mode and 2 MW under forced-convection.

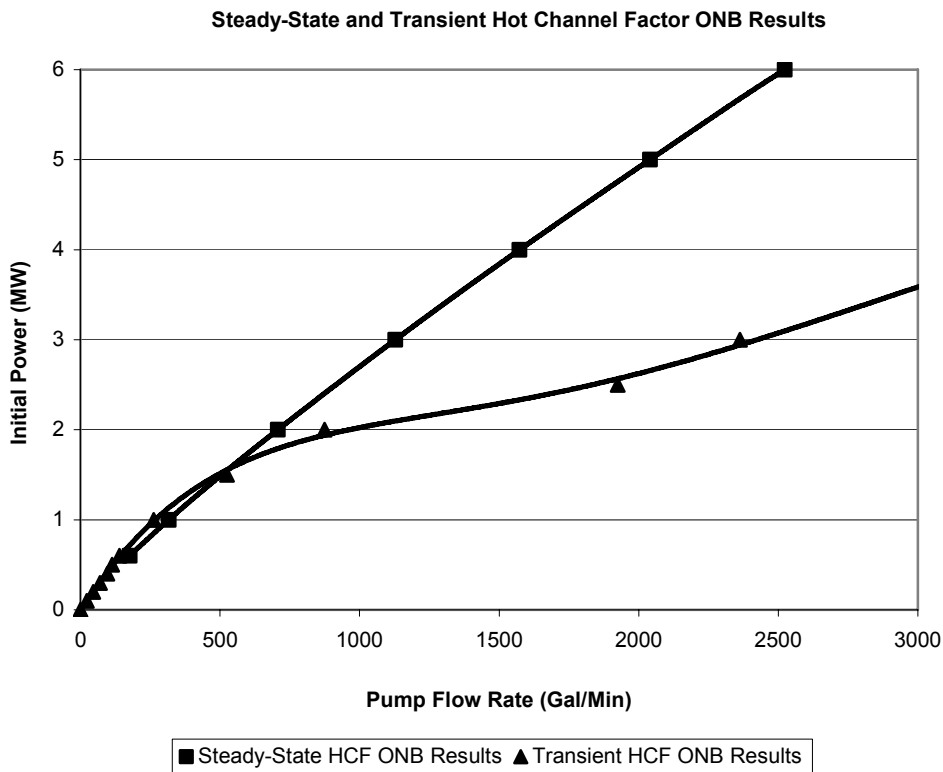


FIG. 4: PLTEMP AND PARET-ANL HOT CHANNEL POWER-TO-FLOW MAPS

TABLE OF CONTENTS

EXECUTIVE SUMMARY	(i-iv)
1.0 INTRODUCTION AND SUMMARY DESCRIPTION	1
1.1 INTRODUCTION	1
1.2 GENERAL DESCRIPTION OF FACILITY	1
1.2.1 Reactor	1
1.2.2 Auxiliary Systems and Radioactive Waste Management	2
1.3 COMPARISON TABLES	2
1.4 IDENTIFICATION OF AGENTS AND CONTRACTORS	2
1.5 REQUIREMENTS FOR FURTHER TECHNICAL INFORMATION	2
1.6 MATERIAL INCORPORATED BY REFERENCE	2
2.0 DETAILED FACILITY DESCRIPTION	3
3.0 REACTOR COMPUTATIONAL MODELS AND CODES	3
3.1 REFERENCE LEU CORE DESIGN	3
3.2 CORE CONFIGURATION CHANGES	5
4.0 NATURAL CONVECTION STEADY-STATE ANALYSIS	10
4.1 NATCON CODE DESCRIPTION	11
4.2 NATCON CODE MODEL (REFERENCE LEU CORE)	12
4.3 NATCON CODE RESULTS (REFERENCE LEU CORE)	14
4.4 NATURAL CONVECTION NITROGEN-16 DISCUSSION AND DATA	15
4.5 TEMPERATURE PROFILE RESULTS	19
5.0 FORCED CONVECTION STEADY-STATE ANALYSIS	20
5.1 PLTEMP CODE DESCRIPTION	20
5.2 PLTEMP CODE MODEL (REFERENCE LEU CORE)	22
5.2.1 Full Core Model (For Pump Flow Distribution)	22
5.2.2 19 Full/2 Partial Element Reference LEU Core	22
5.2.3 Higher Element LEU Cores	23
5.2.4 Hot Channel Model	24
5.3 PLTEMP CODE RESULTS	24
5.3.1 Full Core Model (Pump Flow Distribution) Results	25
5.3.2 Hot Channel Analysis Results	27
6.0 TRANSIENT ANALYSIS	32
6.1 PARET-ANL CODE DESCRIPTION	32
6.2 PARET-ANL CODE MODEL (REFERENCE LEU CORE)	33
6.3 PARET-ANL CODE RESULTS (REFERENCE LEU CORE)	39
6.3.1 Step Reactivity Insertion Results	39
6.3.2 Ramp Reactivity Insertion Results	43
6.3.3 Loss-of-Pump-Flow Results	44
6.3.4 PARET-ANL Power-to-Flow Map	50
7.0 REACTOR ANALYSIS SUMMARY	52
8.0 ADDITIONAL SAFETY ANALYSES	56
8.1 REFUELING ACCIDENT	56
8.2 STEP INCREASE IN REACTIVITY	57
8.3 LOSS OF COOLANT	57

9.0 STANDBY SAFEGUARDS ANALYSIS	57
9.1 ESTIMATION OF CONSEQUENCES OF FISSION PRODUCT RELEASE	57
9.1.1 Dose Calculations	58
9.1.2 Thyroid Doses.....	60
9.1.3 Whole Body Dose Equivalents.....	61

LIST OF TABLES

TABLE 3.1 SUMMARY OF REACTOR DATA	6
TABLE 4.1 CONVERSION TO 21 POINT AXIAL PROFILE FOR CRITICAL (16.5") CASE	13
TABLE 4.2 NATCON RESULTS FOR THE REFERENCE LEU CORE.....	15
TABLE 4.3 NITROGEN-16 POOL-WIDE RESULTS.....	16
TABLE 4.4 NITROGEN-16 RESULTS AT POOL SURFACE DIRECTLY ABOVE REACTOR CORE.....	18
TABLE 5.1 PLTEMP REFERENCE LEU CORE FLOW RESULTS.....	26
TABLE 5.2 PLTEMP FLOW THROUGH FUEL REGION RESULTS.....	26
TABLE 5.3 PLTEMP HOT CHANNEL RESULTS.....	27
TABLE 9.1 QUANTITIES OF IODINE ISOTOPES RELEASED FROM A SINGLE FUEL PLATE	59
TABLE 9.2 QUANTITIES OF INERT GASES RELEASED FORM A SINGLE FUEL PLATE	59
TABLE 9.3 THYROID DOSE EQUIVALENTS (REMS) AT FORTY-EIGHT METERS FROM CONTAINMENT RELEASE POINT FOR GROUND LEVEL RELEASES	60
TABLE 9.4 WHOLE BODY DOSE EQUIVALENTS (REMS) AT FORTY- EIGHT METERS FROM CONTAINMENT RELEASE POINT FOR GROUND LEVEL RELEASES.....	61

LIST OF FIGURES

FIGURE 3.1	REFERENCE LEU CORE	4
FIGURE 3.2	LEGEND FOR LEU CORES	5
FIGURE 4.1	6TH ORDER POLYNOMIAL FIT FOR THE HOT CHANNEL AXIAL POWER PROFILE.....	14
FIGURE 4.2	UMLRR POOL CUTAWAY.....	17
FIGURE 4.3	200-KW TEMPERATURE PROFILES (WITH HOT CHANNEL FACTORS)	20
FIGURE 4.4	200-KW TEMPERATURE PROFILES (WITHOUT HOT CHANNEL FACTORS)	20
FIGURE 5.1	PLTEMP POWER-TO-FLOW MAP	28
FIGURE 5.2	BURNOUT HEAT RATIOS.....	30
FIGURE 5.3	2-MW TEMPERATURE PROFILES (WITH HOT CHANNEL FACTORS)	31
FIGURE 5.4	2-MW TEMPERATURE PROFILES (WITHOUT HOT CHANNEL FACTORS)	31
FIGURE 6.1	2-MW STEP-CHANGE REACTIVITY TRANSIENT POWER PROFILE.....	40
FIGURE 6.2	2-MW STEP-CHANGE HOT CHANNEL PEAK CLADDING TEMPERATURE PROFILE.....	41
FIGURE 6.3	200-KW STEP-CHANGE REACTIVITY TRANSIENT POWER PROFILE.....	42
FIGURE 6.4	200-KW STEP-CHANGE HOT CHANNEL PEAK CLADDING TEMPERATURE PROFILE.....	42
FIGURE 6.5	2-MW RAMP REACTIVITY TRANSIENT POWER PROFILE.....	43
FIGURE 6.6	2-MW RAMP HOT CHANNEL PEAK CLADDING TEMPERATURE PROFILE.....	44
FIGURE 6.7	COMPARISON OF TRUNCATED, EXPONENTIAL, AND LINEAR FLOW LOSS.....	45
FIGURE 6.8	TRUNCATED MASS FLUX PROFILE	46
FIGURE 6.9	TRUNCATED TEMPERATURE PROFILE	46
FIGURE 6.10	LINEAR MASS FLUX PROFILE	47
FIGURE 6.11	LINEAR TEMPERATURE PROFILE	47
FIGURE 6.12	EXPONENTIAL MASS FLUX PROFILE	49
FIGURE 6.13	EXPONENTIAL TEMPERATURE PROFILE	49
FIGURE 6.14	CLADDING TEMPERATURE COMPARISON FOR FLOW LOSS MODELS	50
FIGURE 6.15	PARET-ANL POWER-TO-FLOW MAP	51
FIGURE 7.1	PLTEMP POWER-TO-FLOW MAP.....	53
FIGURE 7.2	PARET-ANL HOT CHANNEL POWER-TO-FLOW MAP	55
FIGURE 7.3	PARET-ANL NATURAL CONVECTION POWER-TO-FLOW MAP	55
FIGURE 7.4	PLTEMP AND PARET-ANL HOT CHANNEL POWER-TO- FLOW MAPS	56

1.0 INTRODUCTION AND SUMMARY DESCRIPTION

1.1 INTRODUCTION

This report presents a description and safety evaluation of the University of Massachusetts Lowell Reactor (UMLRR) fueled with low enrichment fuel (LEU) for an increase in steady state power rating from 1 MW to 2 MW thermal. Comparison of pertinent data for operations at 1 MW and 2 MW thermal is included.

This report is submitted in support of an application for permission to upgrade the steady state power level under License R-125.

1.2 GENERAL DESCRIPTION OF FACILITY

The general description of the facility is unchanged from the current FSAR in terms of history of the facility, location, general housing, reactor building, and backup systems. Some changes have occurred in the reactor core and in some related systems as discussed below.

1.2.1 Reactor

The reactor was originally fueled with an HEU core (U-Al enriched to 93% ^{235}U alloyed with aluminum) and later converted to an LEU core (U_3Si_2 enriched to 19.75% ^{235}U alloyed with aluminum) in August 2000.

Among the various changes from the HEU core configuration, the original LEU reference core design was much smaller and required a complicated modification to the reactor power regulating rod to move it closer to the fuel.¹ Subsequently, a new configuration based upon 21 LEU fuel elements (19 standard and two partial assemblies) was designed and chosen to eliminate the regulating rod modification. In preparation of the conversion and new configuration, an updated set of specific computational models was developed to verify the changes would not affect the approved safety analysis.² After this new configuration was loaded, a complete set of physics tests were undertaken to verify the core performance was within the design parameters submitted in the safety analysis. These results were submitted in the Conversion Report to the NRC.³ This subsequent new configuration is used in this supplemental analysis and is herein referred to as the Reference LEU core.

The core grid plate, consisting of a 9 by 7 rectangular array of spaces in an egg-crate type of bottom plate, is capable of being loaded with fuel, reflector elements (graphite), or experimental radiation “baskets.” The fuel elements for the LEU core are heavily loaded with fissile material (). The Reference LEU core configuration consists of 19 LEU elements and two partial LEU elements (Figure 3.1). This core, although smaller than the original HEU core, has similar fluxes in the fuel because of higher macroscopic cross sections, but provides improved fluxes for experiments. A centrally-located flux trap enhances available thermal fluxes even more. In turn, the smaller core results in slightly lower power limits using the onset of nucleate

boiling criterion at identical coolant flow, but safety analyses show that all credible accidents lead to parameters still well below safety limits (see the analyses in Sections 3.0 through 7.0 of this report).

1.2.2 Auxiliary Systems and Radioactive Waste Management

None of the Auxiliary Systems described in the FSAR are affected by, or will change, as a result of the increased power level.

Liquid, gaseous, and solid radioactive waste or methods of waste treatment are not expected to change significantly as a result of raising the power level of the UMLRR.

1.3 COMPARISON TABLES

The FSAR shows some comparisons in tabular form with research reactors that are rather similar to the UMLRR. These will change somewhat with the elevation of the steady-state power level of the UMLRR, nevertheless, the fundamental reactor concepts are still similar. Detailed comparison is difficult because of the different current status of each reactor affected.

The cross-pool flow mode described in the current FSAR is not affected by the change of power level.

1.4 IDENTIFICATION OF AGENTS AND CONTRACTORS

All calculations of core parameters were accomplished in-house. Assistance was provided in compilation of the license package by Research Reactor Safety Analysis Services.

1.5 REQUIREMENTS FOR FURTHER TECHNICAL INFORMATION

Further technical information beyond that contained in this document is not required for steady-state operation at 2 megawatts thermal.

1.6 MATERIAL INCORPORATED BY REFERENCE

The UML Reactor FSAR and the FSAR Supplement for Conversion to Low Enrichment Uranium (LEU) Fuel are used extensively as references herein.

The new material incorporated by reference includes various internal reports of calculations done at UML, and several theses and topical report papers given at meetings. Much of the safety analysis data and results reported herein came directly from the thesis by Stevens.⁴ The particular references are tabulated in the sections that give detailed information about the power upgrade.

2.0 DETAILED FACILITY DESCRIPTION

Descriptions of the site, containment, and meteorology are not affected by the power upgrade. Much of the facility described in Chapter 4 of the FSAR is also not affected, but core arrangement and associated reactor physics are different. Those changes have been considered in the FSAR Supplement for the Conversion to Low Enrichment Uranium¹ and in other subsequent publications.^{2,3}

3.0 REACTOR COMPUTATIONAL MODELS AND CODES

The majority of the thermal hydraulic analysis on the reference LEU core was completed using three computer codes: NATCON,⁵ PLTEMP,⁶ and PARET-ANL.^{7,8} The most current versions of the codes were obtained from Argonne National Laboratory in late 1999. NATCON is a natural convection steady-state code used to simulate the conditions for natural convection flow in a fuel channel. PLTEMP is a forced convection steady-state code used to simulate pump flow through the entire reactor core, as well as to perform a hot channel analysis. PARET-ANL (an Argonne National Laboratory modification of the original PARET) is a transient code used to simulate rapid reactivity changes in the reactor core and loss of flow scenarios. All three of the computer codes are input file driven, requiring the development of appropriate input files in order to simulate the reference LEU core and a variety of off-normal situations. Many of the cases were run at low power levels of 100 and 200 kilowatts, and high power levels of 1 and 2 MW, in order to simulate the actual and proposed natural and forced convection limits, respectively.

The overriding concern of a power upgrade is the safety of the public, which is achieved by operating the reactor well below its safety limit. The onset of nuclear boiling (ONB) is the licensed technical specification safety limit for the reactor. The safety limit of ONB provides a significant margin of safety far below the temperature at which fuel cladding damage may occur. The fuel cladding is the primary barrier of multiple safety barriers designed to prevent or limit fission product releases to the environment. In addition, the reactor must be operated in a mode well below the ONB due to uncertainties involved in the measurement of key parameters, such as flow, heat flux, and the heat transfer coefficient. The safety margin is preserved further by the use of Limited Safety System Settings (LSSS). Original LSSS criteria are stipulated in the Final Safety Analysis Report (FSAR) of the UMLRR.⁹ New LSSS criteria for a 2-MW core are discussed in the PARET-ANL section.

3.1 REFERENCE LEU CORE DESIGN

As mentioned previously, a decision was made to design a new LEU core configuration that would not require a mechanical alteration of the regulating rod. The current LEU core configuration consists of 19 LEU elements of the same description as earlier, with an additional 2 partial LEU elements with one-half the fuel loading of a full

element. This 19 full/2 partial-element core is the reference LEU core design that the thermal hydraulic analysis is based on.

Geometrically, there are a few differences between this design and the original 20-element LEU design. Two of the five normal radiation baskets used for in-core experiments were removed. This allowed for the additional fuel element, and an additional graphite reflector. The central flux trap remained. The two partial fuel elements were located directly between the control blades and the central flux trap. This allowed for a more even burnup of fuel. The regulating rod position was maintained in its original D-9 position in the HEU core. The reference LEU core is shown in Figure 3.1. A summary of the physics and thermal hydraulics data for the reference core at 1 MW and 2 MW is provided in Table 3.1.

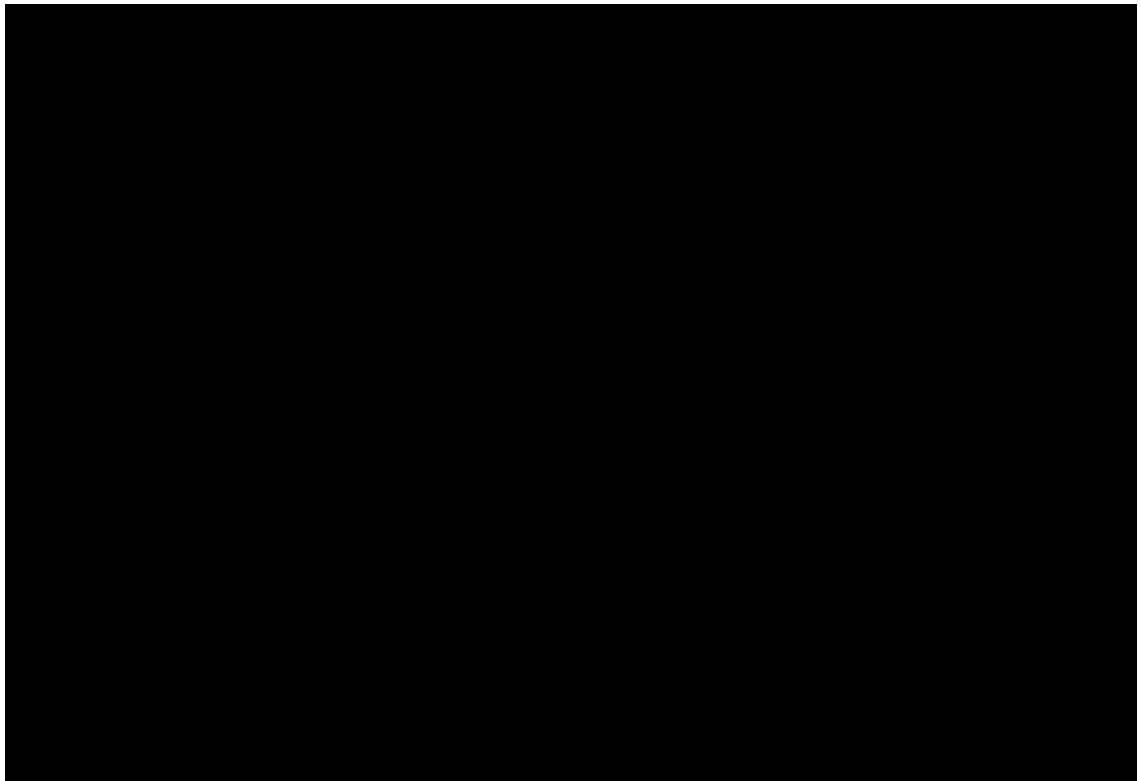


FIGURE 3.1: REFERENCE LEU CORE (SEE FIGURE 3.2 FOR LEGEND)

3.2 CORE CONFIGURATION CHANGES

To date, there have been some changes made from the reference LEU core configuration. The first was the movement of the four flooded and capped radiation baskets two grid positions outward to the edge of the core, switching positions with graphite reflectors. This was done to optimize the core reactivity for long-term operations. This minor change had a negligible effect on the thermal hydraulic analysis. In particular, reactor physics analysis by J. Byard¹⁰ had the total peaking factor for this core configuration slightly lower than the reference LEU core. Therefore, since the total peaking factor went down, conservatism is maintained, and the reference LEU core configuration thermal hydraulic analysis is valid for this core.

A fast neutron irradiator (FNI) facility has been installed along one side of the reactor core. The major changes to the 9x7 core grid were the movement of the neutron source from A-5 to G-5 and the replacement of the five graphite reflectors in A-3 through A-7 with voided lead baskets adjacent to the FNI. Although the flux profiles are shifted somewhat for this configuration relative to the reference core, analysis by J. R. White, et al.¹¹ shows little change in the radial and axial peaking factors. Thus, the reference LEU core thermal hydraulic analysis applies to this new configuration.

Since changes in the operating configuration of the UML research reactor are common, the thermal analysis of the reference LEU core has enough of a safety margin built into it to allow for a variety of anticipated minor changes in the core structure, such as those described above. Configuration changes such as these should fall within the uncertainty limits imposed on the current analyses. Anticipated minor changes in the LEU core include replacement of fuel elements due to burnup, rotation of elements axially and radially, and radiation basket changes that do not involve flow changes.

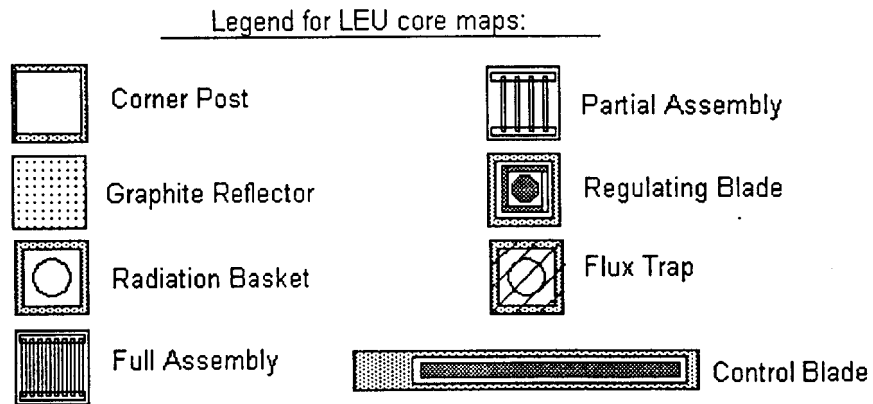


FIGURE 3.2: LEGEND FOR LEU CORES

TABLE 3.1. SUMMARY OF REACTOR DATA

	<u>1-MW DATA</u>	<u>2-MW DATA</u>
<u>Purpose of Reactor</u>	Education and Research	No change
<u>Location of Reactor</u>	Lowell, Massachusetts	No change
<u>Reactor Materials</u>		
Fuel	Uranium Silicide (19.75% ²³⁵ U)	No change
Moderator	High-purity water	No change
Reflector	Graphite and water	No change
Coolant	High-purity water	No change
Control	Boral	No change
Structural Material	Aluminum	No change
Shield	Concrete and water	No change
<u>Dimensions</u>		
Core (active section)	19 full and 2 partial fuel elements [REDACTED] [REDACTED] with a central flux trap irradiation zone	No change
Reflector	3 in. square; 30 in. high	No change
Grid Box	9 x 7 array of 3 in.-square modules	No change
<u>Fast (above 1 eV) and Thermal (below 1 eV) Fluxes at Rated Power for Reference Cores</u>		
Maximum thermal neutron flux in the fuel (D6 lower left)	1.7 x 10 ¹³ nv	3.4 x 10 ¹³ nv
Average thermal neutron flux in the fuel (D7 center)	1.1 x 10 ¹³	2.2 x 10 ¹³
Maximum thermal neutron flux in the central flux trap (D5 center)	3.0 x 10 ¹³	6.0 x 10 ¹³

TABLE 3.1. SUMMARY OF REACTOR DATA (Continued)

	<u>1-MW DATA</u>	<u>2-MW DATA</u>
Maximum fast neutron flux in the central flux trap (above 1 eV)	3.9×10^{13}	7.8×10^{13}
Average fast neutron flux in the fuel (D7 center)	3.2×10^{13}	6.4×10^{13}
Maximum fast neutron flux in the central flux trap (D5 center)	3.0×10^{13}	6.0×10^{13}
<u>Reference Core Parameters</u>		
Clean, cold core loading	██████████ (19 full and 2 partial elements)	No change
Operating excess reactivity	2.95% $\Delta k/k$	No change
Reactivity in safety blades	11.6% $\Delta k/k$	No change
Shutdown margin with one stuck blade	4.70% $\Delta k/k$	No change
Temperature coefficients:		
Coolant Temperature	$-0.48 \times 10^{-4} \Delta k/k/^{\circ}C$	No change
Fuel Doppler	$-0.15 \times 10^{-4} \Delta k/k/^{\circ}C$	No change
Total Temperature Coeff.	$-0.63 \times 10^{-4} \Delta k/k/^{\circ}C$	No change
Void Coeff.	$-2.36 \times 10^{-3} \Delta k/k/\% \text{Void}$	No change
Prompt neutron generation time, Λ	$6.45 \times 10^{-5} \text{ sec}$	No change
β_{eff}	0.0078	No change
<u>Thermal Characteristics (based on 20 elements)</u>		
Heat Output	1 MW (th)	2 MW (th)
Hot channel factors (HCFs)	F_q : heat flux uncertainty = 1.25	No change
	F_b : uncertainty in bulk flow or enthalpy change in a channel = 1.24, and	No change

TABLE 3.1. SUMMARY OF REACTOR DATA (Continued)

	<u>1-MW DATA</u>	<u>2-MW DATA</u>
Hot channel factors (HCFs) (cont.)	F_h : the uncertainty in the heat transfer process = 1.35	No change
Maximum heat flux	27,500 BTU/h-ft ²	51,000 BTU/h-ft ²
Specific power (clean, cold)	250 watts/gm ²³⁵ U	500 watts/gm ²³⁵ U
Maximum gamma heat in core	1.5 watts/cc	3.0 watts/cc
Maximum coolant flow rate	2,000 gpm	No change
Coolant flow velocity (in fuel channel at maximum flow rate)	3.9 ft/sec.	No change
Maximum water intake temperature (hot channel at rated power)	43 °C	No change
Maximum fuel temperature (max flow, rated power with HCFs)	62.1 °C	79.5 °C
Maximum clad temperature (max flow, rated power with HCFs)	61.8 °C	78.9 °C
Maximum water temperature (max flow, rated power with HCFs)	48.5 °C	54.0 °C
Average coolant ΔT at rated power and maximum flow (no HCFs)	1.9 °C	3.8 °C
ONB flow rate at rated power with HCFs	316 gpm	707 gpm
Clad temperature at ONB flow	120 °C	No change
Primary water pressure at heat exchanger	50 psig	No change
Secondary water pressure at heat exchanger	35 psig	No change
Pressure drop through core at maximum flow rate	0.4 psi	No change

TABLE 3.1. SUMMARY OF REACTOR DATA (Continued)

	<u>1-MW DATA</u>	<u>2-MW DATA</u>
<u>Control</u>		
Safety elements	Four 10.6 inch wide vertical blades	No change
Regulating elements	One 2.5 inch square vertical rod	No change
Composition	Boral (min 35 wt% boron)	No change
Withdrawal rate of safety blades	3.5 inches/minute	No change
Withdrawal rate of regulating rod	78 inches/minute	No change
<u>Fuel Assembly Details</u>		
Type	Plate	No change
Number of elements	19 full + 2 partial	No change
Number of fuel plates per element	16	No change
Plate thickness	0.1270 cm	No change
Clad thickness (full element)	0.0380 cm	No change
Plate width	████████	No change
Plate length	████████	No change
Active fuel length	████████	No change
Active fuel width	████████	No change
Water gap	0.2963 cm	No change
Over-all element length	████████	No change
Cladding	Aluminum	No change
Fuel alloy	U ₃ Si ₂ -Al	No change
²³⁵ U/element	████████	No change

TABLE 3.1. SUMMARY OF REACTOR DATA (Continued)

	<u>1-MW DATA</u>	<u>2-MW DATA</u>
<u>Reactivity Requirements</u>	($\Delta k/k$) at 1 MW _t	($\Delta k/k$) at 2 MW _t
Equilibrium Xenon (based on Single daily 8-hr shift)	2.2 %	3.0 %
Temperature	0.1 %	0.1 %
Fuel burnup, experiments	2.2 %	1.4 %
Total	4.5%	4.5%
<u>Design and Operating Characteristics</u>		
Void coefficient	Negative	No change
High flux scram limit	125 % rated	115 % rated
Maximum excess reactivity	4.7 % $\Delta k/k$	No change
Maximum worth of regulating rod	$< \beta_{\text{eff}}$	No change
Normal range of blade worths	2.4 % $\Delta k/k$ to 3.4 % $\Delta k/k$	No change
Total worth of 4 control blades	11.6% $\Delta k/k$	No change
Maximum single sample worth	0.5% $\Delta k/k$	No change
Startup count rate, minimum	2 counts/second	No change

4.0 NATURAL CONVECTION STEADY-STATE ANALYSIS

This section describes the NATCON code used to perform the natural convection steady-state thermal hydraulic analysis on the reference LEU core, the parameters modeled from the reference LEU core used in the NATCON code input files, and the results obtained from the NATCON code output. This section also includes a discussion of the effects that Nitrogen-16 has on choosing a natural convection operating power limit. Experimental data for Nitrogen-16 dose rates attributable to several natural convection power levels are also presented.

4.1 NATCON CODE DESCRIPTION

The NATCON computer code,⁵ developed by Argonne National Laboratory, was created as a tool to simulate the thermal hydraulics of plate-type research reactors under natural convection cooling. The code assumes that the fuel elements are immersed in a standing pool of water at an average, constant temperature. Buoyancy forces are exerted on a column of water at the ambient temperature when the coolant is heated in a channel. A pressure drop is realized when these buoyancy forces are resisted by frictional forces. Natural convection then occurs as a steady-state condition. The Darcy-Weisbach expression⁵ is used to estimate the wall friction, with exit and entrance loss effects contributing to the frictional forces. Fuel, clad, and coolant axial temperature distributions and the coolant flow rate are computed by the code once the steady-state condition is reached.

The NATCON code has two modes of operation. The above parameters can be computed using a fixed input power level, or the power level can be automatically incremented until the ONB power level is obtained. The Bergles-Rohsenow correlation⁵ is used to compute the ONB heat flux, and is shown below.

$$q_{\text{ONB}} = (1.0829 \times 10^{-3}) P^{1.156} (1.8 \Delta T_{\text{sat ONB}})^{2.16/[P^{(0.0234)}]}$$

$$q_{\text{ONB}} = \text{heat flux at ONB (MW/m}^2\text{)}$$

$$P = \text{pressure (bars)}$$

$$\Delta T_{\text{sat}} = (T_{\text{wall}} - T_{\text{sat}}) (\text{°C})$$

NATCON requires the input of the physical characteristics of the fuel elements, such as dimensions, densities, and thermal conductivities. Other inputs are the temperature of the pool, the location of the elements from the top of the pool, the radial peaking factor of the elements, and the axial flux profile within the elements. NATCON also includes safety margins, referred to as hot channel factors, to model uncertainties in the heat flux, flow rate, and heat transfer, which add conservatism to the model. An initial guess as to the coolant velocity is also needed in the input file.

Based on these input parameters, NATCON calculates the flow rate, the axial temperature distribution at the fuel centerline, fuel plate surface, and coolant channel, as well as the power level associated with the ONB point. ONB is used as the thermal hydraulic criterion for determining if the reactor is operating safely. It adds an additional element of conservatism to the operation of a research reactor, as the thermal hydraulic criterion for commercial power reactor safety analyses is departure from nucleate boiling (DNB).

4.2 NATCON CODE MODEL (REFERENCE LEU CORE)

The following paragraphs provide a description of many of the key parameters used in NATCON to obtain a steady-state natural convection limit for the UMLRR.

The number of axial regions chosen in the reactor coolant channel was 20, which allowed for 21 points in the axial profile of the power density input from reactor inlet to outlet. This axial power density profile was determined from reactor physics data,² and represents a critical height of 16.5 inches withdrawn for all of the control blades. This control blade height was determined to be the most limiting case, compared to a fully-withdrawn profile. The 16.5-inch profile is significantly bottom-peaked, and has a higher axial peaking factor than the fully-withdrawn profile. The axial profile for the hot channel, as opposed to the average channel, was used to provide conservatism to the model, as it has a larger peak-to-average power ratio along the channel. The conversion from raw reactor physics data to the 21-point normalized axial power density profile, which is the maximum number of points allowable for NATCON, is shown in Table 4.1. The z-axis origin for NATCON is the inlet (bottom) of the reactor with natural convection flow in the upward direction from the bottom to the top of the core.

A sixth order polynomial fit was applied to the raw reactor physics data, which had 27 axial nodes in the core region, in order to generate a curve to obtain the 21 axial node points for use in NATCON. This curve is shown in Figure 4.1 with the polynomial fit.

Due to the limitation of the NATCON code to model only one type of fuel element, a decision was made to count the two partial fuel elements as one full element, making 20 full fuel elements the basis of the model. This was only done for the NATCON code, and also adds a slight conservatism to the model by increasing the average power density per element. Sixteen fuel plates per element were modeled, as the 2 end plates contain no fissile material. This was necessary as NATCON only allows one type of plate to be modeled, and since the end plates generate no heat, this was not seen as a limitation in the model.

TABLE 4.1: CONVERSION TO 21-POINT AXIAL PROFILE FOR CRITICAL (16.5") CASE

Conversion to 21 Point Axial Profile for Critical (16.5 ") Case					
Node	Reference	Normalized	21 Point	21 Point	21 Point
Width	Height	Axial	Reference	Normalized	Normalized
(cm)	(cm)	Profile	Height	Reference	Axial
			(cm)	Height	Profile
2.4817	1.2409	0.7812	0.0000	0.0000	0.7669
2.4817	3.7226	0.8154	2.9845	0.0500	0.8084
2.4817	6.2043	0.9149	5.9690	0.1000	0.9070
2.4667	8.6785	1.0226	8.9535	0.1500	1.0274
2.4667	11.1452	1.1221	11.9380	0.2000	1.1454
2.4667	13.6119	1.2077	14.9225	0.2500	1.2455
2.0000	15.8452	1.2700	17.9070	0.3000	1.3188
2.0000	17.8452	1.3139	20.8915	0.3500	1.3614
2.0000	19.8452	1.3454	23.8760	0.4000	1.3730
2.0000	21.8452	1.3644	26.8605	0.4500	1.3554
2.0000	23.8452	1.3707	29.8450	0.5000	1.3120
2.0000	25.8452	1.3645	32.8295	0.5500	1.2463
2.0000	27.8452	1.3459	35.8140	0.6000	1.1625
2.0000	29.8452	1.3156	38.7985	0.6500	1.0643
2.0000	31.8452	1.2743	41.7830	0.7000	0.9554
2.0000	33.8452	1.2229	44.7675	0.7500	0.8399
2.0000	35.8452	1.1629	47.7520	0.8000	0.7228
2.0000	37.8452	1.0959	50.7365	0.8500	0.6104
2.0000	39.8452	1.0239	53.7210	0.9000	0.5121
2.0000	41.8452	0.9491	56.7055	0.9500	0.4411
2.0000	43.8452	0.8729	59.6900	1.0000	0.4163
2.4667	46.0786	0.7877			
2.4667	48.5453	0.6950			
2.4667	51.0120	0.6052			
2.4817	53.4862	0.5207			
2.4817	55.9679	0.4495			
2.4817	58.4496	0.4213			

Of particular note is that the average temperature of the water was designated at 43° C, which is the current safety limit of the UMLRR, and well above the average operating temperature of 20° C. This adds conservatism to the model due to the fact that a higher heat flux would need to exist at the lower operating temperature to reach the ONB.

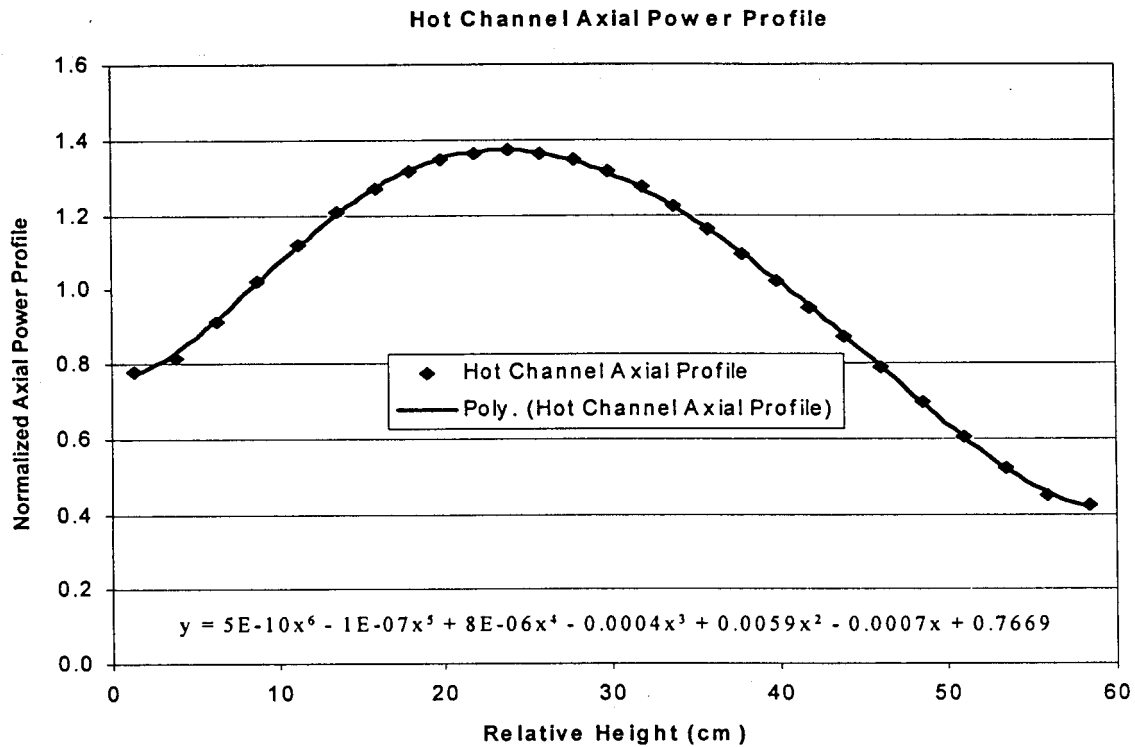


FIGURE 4.1: 6TH ORDER POLYNOMIAL FIT FOR THE HOT CHANNEL AXIAL POWER PROFILE

The NATCON analysis was done twice, once with engineering hot channel factors, and once without. This was done to see how much conservatism the engineering hot channel factors add to the model, as well as to compare the results to previous data for both the HEU core and the originally-designed LEU core. Engineering hot channel factors represent the uncertainty in the model associated with the flow rate, heat flux, and heat transfer coefficient. These engineering hot channel factors consisted of a flow uncertainty value of 1.24, a heat flux uncertainty value of 1.25, and a heat transfer coefficient uncertainty of 1.35. A value of unity represents no uncertainty. The methodology of arriving at these specific engineering hot channel factors is described in the FSAR Supplement.¹

4.3 NATCON CODE RESULTS (REFERENCE LEU CORE)

The ONB point for the case without engineering hot channel factors was determined to be 622 kW. This result compares favorably with the original LEU design result of 598 kW. The higher value is attributed to the larger number of fuel plates. When engineering hot channel factors were added, there was some difficulty getting the code to converge. Therefore, by manually inputting the reactor power to determine how close to ONB the reactor came, convergence was eventually reached. By approaching from above and below, the ONB power level was determined to lie between 392 kW and

393 kW, so the value of 392 kW was used. This result compares favorably with the original LEU design result of 335 kW, since a slightly higher margin to ONB due to the lower peaking factors was expected. The case without engineering hot channel factors has a much higher power level margin to ONB due to modeling 100% certainty in the values of power, flow, and the heat transfer coefficient. A summary of the results of the NATCON analysis is shown in Table 4.2.

TABLE 4.2: NATCON RESULTS FOR THE REFERENCE LEU CORE

NATCON Results					
Hot Channel Factors	ONB Power kW	Max Clad Temp deg C	Max Plate Power kW	Outlet Temp deg C	Outlet Velocity cm/sec
No	622	119	2.64	75.0	10.32
Yes	392	123	2.09	77.2	7.64

The current Limited Safety System Setting (LSSS) of the UMLRR during natural convection operation is 125 kW,¹² which corresponds to a 25% greater than maximum natural convection power level of 100 kW. Due to reactor power instrumentation being on a decade scale, increasing to a maximum full power level of 2 MW would likely necessitate an accompanied parallel increase to a maximum natural convection power level of 200 kW. An alarm setpoint of 105%, a scram setpoint of 110%, and an LSSS of 115% are anticipated for operation of a 200 kW natural convection core (and 2-MW forced-convection core). The corresponding LSSS for this new natural convection maximum power level would then be 230 kW. The margin to ONB from the LSSS based on the NATCON results would be at least a factor of 1.7 for steady-state conditions, including all of the conservatism built into the model. Therefore, based on the NATCON results, the reactor could be operated safely at 200 kW in natural convection from a steady-state thermal hydraulic standpoint. This result is subject to both a Nitrogen-16 analysis, due to concerns about dose rates to the general public during reactor tours while the reactor is operating in natural convection mode, as well as the results from the PARET-ANL reactivity transient analysis discussed in Section 6.0.

4.4 NATURAL CONVECTION NITROGEN-16 DISCUSSION AND DATA

The Technical Specifications of the UMLRR stipulate that the radiological dose Nitrogen-16 from the pool surface during natural convection operations shall be minimized to the greatest extent possible. Nitrogen-16 is produced from a fast neutron reaction with Oxygen-16. The products of that reaction are the Nitrogen-16 itself as well as a proton (ionized Hydrogen-1). Nitrogen-16 has a half-life of approximately seven seconds, but it gives off extremely energetic gamma rays when it decays. A holdup tank was designed on the primary system to stall the water with baffles for 2 minutes to allow for the Nitrogen-16 to decay during forced convection operations. The holdup tank also

has a vent on top to exhaust the hydrogen gas buildup due to the hydrogen atoms covalently-bonding to form a diatomic gas. However, during natural convection operations, some of the Nitrogen-16 will escape from the pool surface before it all decays. This historically has been the reason the LSSS was set at 125 kW for natural convection operations, in lieu of the thermal hydraulic natural convection results.

Prior to the installation of the reference LEU core, experimental data were gathered during operation of the HEU core in natural convection mode. An extremely sensitive ion chamber which measured field readings in the microrem range was used to determine the dose rate from the Nitrogen-16 at the surface of the pool. Measurements were initially taken at six different points all around the reactor pool at the natural convection power limit of 100 kW, including directly over the reactor core. It was predicted that natural convection circulation patterns in the water would cause the Nitrogen-16 to migrate across the pool. A background average dose rate of 15 microrems per hour was measured inside containment prior to startup, to use as a reference point. The results of this experiment are shown in Table 4.3.

TABLE 4.3: NITROGEN-16 POOL-WIDE RESULTS

Experiment Performed 11/99 To Quantify N-16 Dose Rates Near Surface Of Pool In 6 Different Locations Around Reactor Pool At 100 kW						
Detector Used: Bicron MicroRem						
Serial #: B362A						
Last Calibrated: 8/99						
Data Taken Every 5 Minutes At 100 kW (0 - 60 Minutes Inclusive)						
Baseline: 15 microR/hr (Background)						
Positions Proceed Clockwise Around Reactor Pool As Follows:						
Position 1: Directly Above Center Of Reactor Core						
Position 2: Side Of Pool Near Pool Gate Nearest To Control Room						
Position 3: Side Of Pool Near Bulk Pool End Nearest To Control Room						
Position 4: At Bulk Pool Detector						
Position 5: Side Of Pool Near Bulk Pool End Furthest From Control Room						
Position 6: Side Of Pool Near Pool Gate Furthest From Control Room						
Time in Minutes	Dose Rate in microR/hr					
	Position 1	Position 2	Position 3	Position 4	Position 5	Position 6
0	300	125	20	20	30	140
5	350	135	80	30	60	140
10	400	150	90	70	85	225
15	400	160	100	95	90	180
20	350	145	100	80	90	160
25	500	200	100	90	90	165
30	425	225	90	80	95	190
35	300	180	105	95	100	160
40	300	150	105	90	110	190
45	350	145	110	100	110	180
50	300	170	110	110	100	200
55	325	190	120	100	115	200
60	350	200	120	105	100	190
Average	358	167	96	82	90	178

As seen from the data in the table, natural convection flow patterns were established, resulting in a large difference in dose rates at different points around the pool due to the Nitrogen-16. It can be seen that the longer the reactor was in operation, the higher the dose rate became at the bulk end of the pool. Also, symmetry was seen across the width of the pool, as both the near and far control room sides showed similar dose rates. The positions start at the pool surface above the core shown in the UMLRR Pool Cutaway in Figure 4.2, and proceed clockwise around the pool.

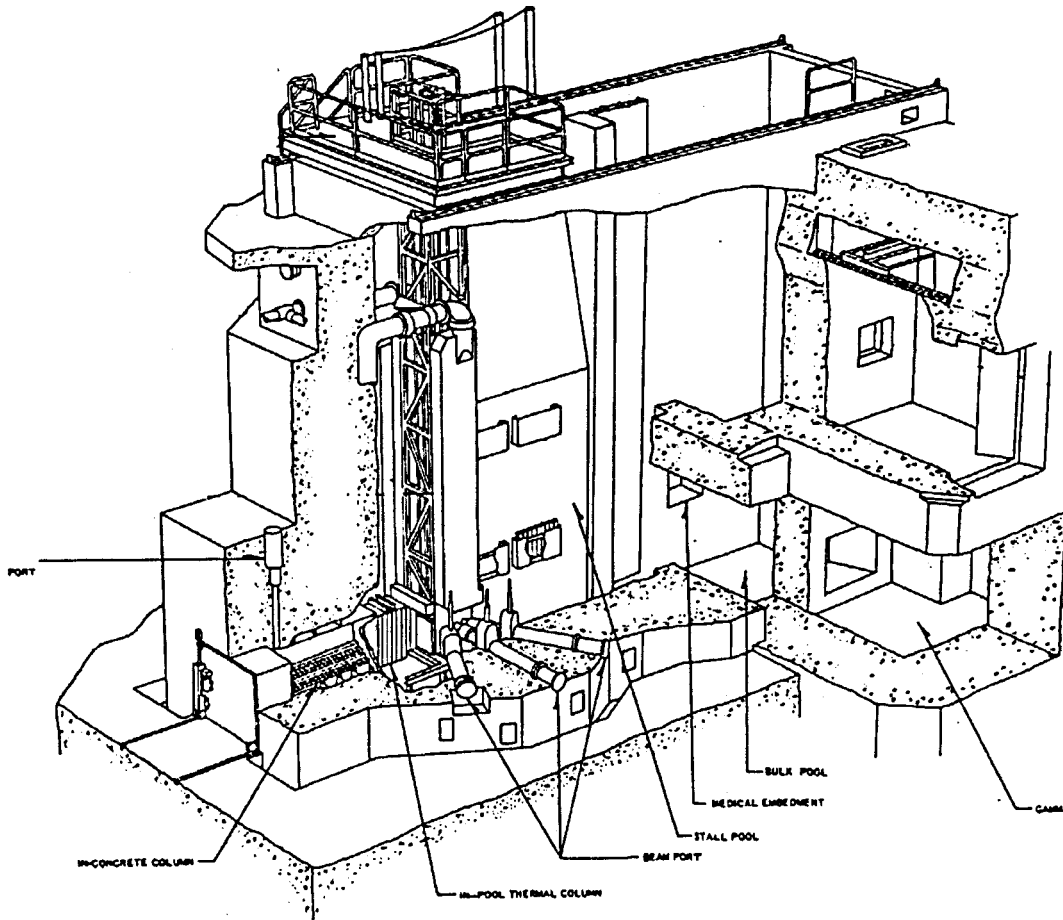


FIGURE 4.2: UMLRR POOL CUTAWAY

The experiment was run again, after the reactor was at power for a short time, for two different natural convection power levels, 25 kW and 50 kW. Data were gathered solely above the reactor core, just slightly above the water level by tying a rope to the detector and then suspending it over the core from the reactor bridge. Readouts were taken from that distance. These data were then compared to the 100 kW over core data to see the effect that the power level had on the dose rate. A rough linear behavior was expected, due to the Nitrogen-16 concentration being proportional to reactor power. Those results are shown in Table 4.4.

**TABLE 4.4: NITROGEN-16 RESULTS AT POOL SURFACE
DIRECTLY ABOVE REACTOR CORE**

Time in Minutes	Power Level		
	25 kW	50 kW	100 kW
0	20	150	300
5	60	150	350
10	85	200	400
15	95	200	400
20	80	250	350
25	75	200	500
30	100	200	425
35	85	150	300
40	75	150	300
45	70	150	350
50	80	150	300
55	75	225	325
60	85	150	350
Average:	76	179	358
	Dose Rate in micro R/hr		

The average dose rate recorded was 76, 179, and 358 microrem per hour for each power level, respectively. The results exhibit an approximately linear behavior, which was expected. An unrestricted area, where members of the general public may enter, is limited to 2 millirem in one hour.¹³ The Nitrogen-16 dose rate at the pool level will peak directly above the center of the core, as this is where the maximum flux in the core is occurring. Therefore, these results are valid for both the reference and current LEU cores, since the maximum flux for all cores is approximately at the center. Based upon the average of approximately 350 microrem per hour, it is theorized that for operation at 200 kW, average Nitrogen-16 dose rates would be approximately 700 microrems per hour. The peak rate is estimated at being right about 1 millirem per hour, since the largest observed value at any time for a power level of 100 kW was 500 microrems per hour, and the increase in dose rates seems to be approximately linear. The legal limit of 2 millirems in one hour represents a factor of two over the theoretical peak value of 1 millirem per hour at 200 kW. Also, the location above the reactor core at pool level is not normally accessible to the general public, and only to reactor staff and researchers performing experiments in the reactor who are classified as radiation workers. Therefore, Nitrogen-16 production is not seen as an impediment to increasing the maximum natural convection steady-state operating power level limit to 200 kW.

4.5 TEMPERATURE PROFILE RESULTS

The final part of the natural convection steady-state analysis was to examine how the temperature of the fuel, cladding, and coolant varied axially as flow progressed through the core. These data were obtained from the hot channel analysis at several natural convection power levels, both with and without hot channel factors, at the NATCON calculated natural convection flow rate. The key results for the nominal 200 kW natural convection case are displayed in Figures 4.3 and 4.4. The fuel and cladding temperatures for all cases increased steadily, coming to a maximum about half-way along the channel, and then decreased somewhat near the top of the core. Recall that the flux/power distribution is slightly bottom-peaked and that flow in the natural convection cases is from the bottom (inlet) to the top (outlet) of the core.

In general, there was less than a one degree Celsius difference between the fuel and cladding temperatures along the entire length of the fuel plate, as seen by the overlapping of the two curves on the graphs. This is due to the fact that the fuel plate is very thin, and the fuel and clad materials have relatively high thermal conductivities. The coolant temperature increased monotonically, as expected, in all cases.

The differences for the cases with and without hot channel factors were significant. For example, for the 200 kW natural convection case, in comparing with and without hot channel factors, the peak fuel and cladding temperatures differed by approximately 16° C between the two cases, while the peak coolant temperature varied by about 6° C.

With hot channel factors, the maximum cladding temperature for the 200 kW natural convection case was less than 90° C. This is significant due to the fact that ONB does not occur during steady-state natural convection conditions until a clad surface temperature of approximately 120° C is reached. Thus, there is a significant safety margin at 200 kW natural convection operations.

Note that the case with hot channel factors does not represent expected behavior during normal operations: it represents a worst-case scenario. The expected best-estimate behavior is represented by the curves in Figure 4.4 that do not include the hot channel factor uncertainties. These results, with and without hot channel factors, clearly show that the UMLRR can be operated safely during steady-state natural convection operations at 200 kW.

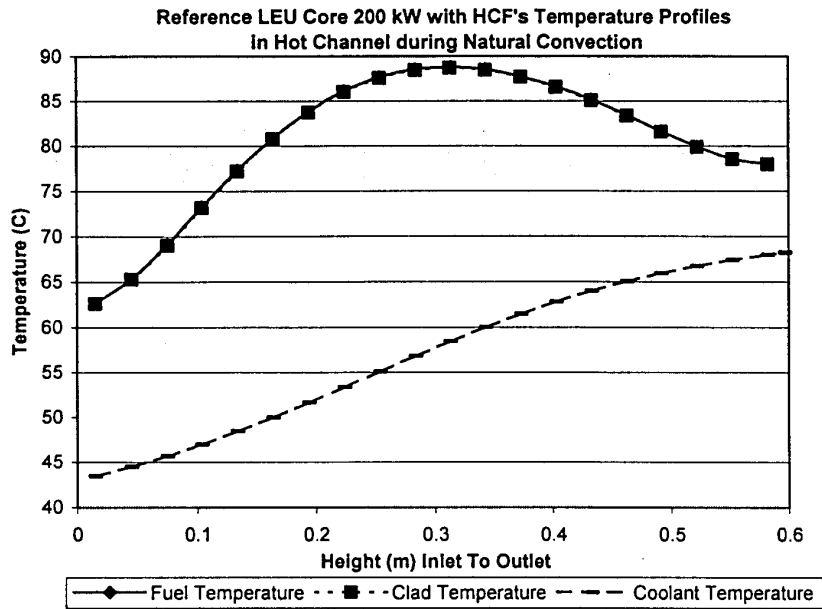


FIGURE 4.3: 200-KW TEMPERATURE PROFILES (WITH HOT CHANNEL FACTORS)

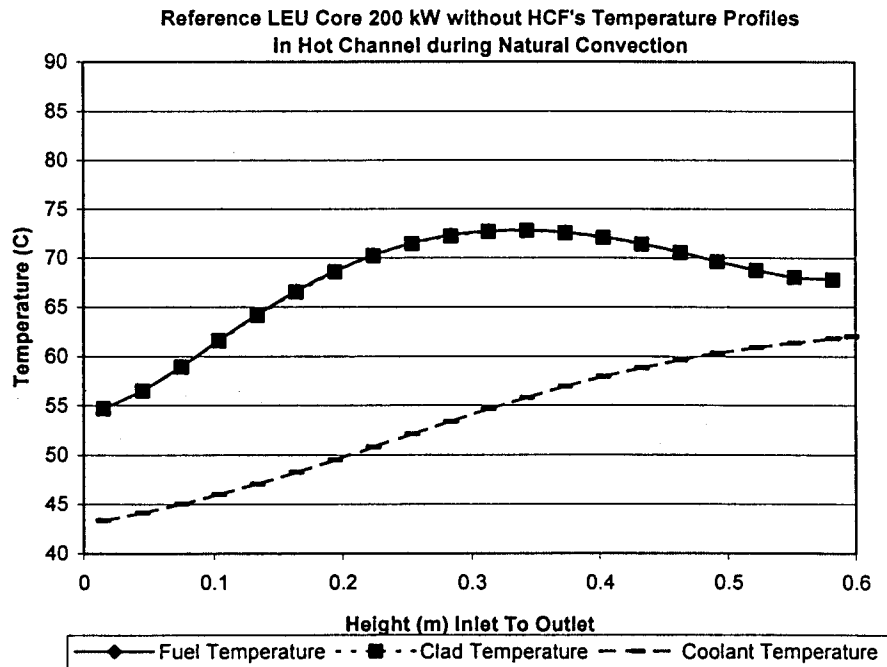


FIGURE 4.4: 200-KW TEMPERATURE PROFILES (WITHOUT HOT CHANNEL FACTORS)

5.0 FORCED CONVECTION STEADY-STATE ANALYSIS

This section describes the PLTEMP code used to perform the forced convection steady-state thermal hydraulic analysis on the reference LEU core, the parameters modeled from the reference LEU core used in the PLTEMP code input files, and the results obtained from the PLTEMP code output. Results are included for both a full-core model and a hot channel analysis. The full-core model was used to determine the percentage of total core flow through the fuel channels, and includes results for both the reference 19 full/2 partial-element LEU core and higher-element cores. Higher-element cores were examined to see how the core flow distribution changes by adding additional elements to the LEU core due to fuel burnup. The hot channel model was used to determine the power-to-flow operating envelope of the reactor during forced convection steady-state operations. Burnout heat ratios and various temperature profiles were also obtained from the hot channel model.

5.1 PLTEMP CODE DESCRIPTION

The PLTEMP computer code, developed by Argonne National Laboratory, was created as a tool to simulate the thermal hydraulics of plate-type research reactors under forced convection cooling. A single hot channel can be modeled, or up to five different fuel element types may be modeled concurrently, each with up to 30 individual elements and 29 fuel plates per element (30 flow channels). Five different types of flow bypasses, such as control blades and radiation baskets, can also be modeled.

The channel flow rate that imposes a common pressure drop across all the flow paths is iterated by the code until the flow distribution through the core is determined. Since it was assumed that the ONB point was not reached under normal operating conditions, only the pressure drops for single-phase flow are computed. In a similar manner, the flow distribution through all of the fuel coolant channels is also calculated. At each prescribed core pressure drop, the flow rates are determined. Once the steady-state flow distribution and heat generation are computed, the code employs a nodalized axial flow model and the 1-D heat conduction equation to compute coolant, cladding, and fuel temperatures. Three different heat transfer correlations are provided by the code to allow the single-phase heat transfer coefficient to be calculated. The critical heat flux is also predicted using the temperature and flow results for each channel. PLTEMP provides boiling regime indications through the Jens-Lottes² correlation for predicting bulk boiling and the Bergles-Rohsenow² correlation for predicting the ONB. The Bergles-Rohsenow correlation was described in the NATCON section. The Jens-Lottes correlation is shown below.

$$q_{\text{sat}} = e^{(2P/31)} \times (\Delta T_{\text{sat}}/25)^4$$

$$q_{\text{sat}} = \text{flux at saturated bulk boiling (MW/m}^2\text{)}$$

$$P = \text{pressure (bars)}$$

$$\Delta T_{\text{sat}} = T_{\text{sat}} - T_{\text{coolant}} (\text{°C})$$

This correlation is applicable to research reactors, which typically operate at low temperatures and pressures. The coolant velocities, axial temperature profiles, critical heat fluxes, and other parameters are included in the code output, as well as the flow distribution in the core and bypass channels.

PLTEMP requires the input of the physical characteristics of the fuel elements, such as dimensions, densities, and thermal conductivities, as well as the dimensions of the flow bypass channels. Entrance and exit friction loss coefficients, the radial peaking factor for each fuel plate, the normalized axial power density profile, the operating power level, and the water pressure and temperature are also required. PLTEMP also includes the same safety margins as NATCON, known as engineering hot channel factors, to model uncertainties in the heat flux, flow rate, and the heat transfer coefficient in the input parameters.

Based upon these input parameters, PLTEMP calculates the flow rate in each of the different flow paths (elements and bypasses) for various pressure drop values. From this, the flow distribution for each channel is calculated. Coolant and fuel plate temperature changes are also tracked. Heat flux data are used to determine whether the flow regime has switched from single phase to the ONB flow regime.

5.2 PLTEMP CODE MODEL (REFERENCE LEU CORE)

The following subsections describe the input parameters used to model the reference UMLRR LEU core during forced-convection steady-state operations. A full core model to determine the flow distribution, as well as a hot channel model, were developed.

5.2.1 Full Core Model (For Pump Flow Distribution)

The full core model was used to determine the percentage of total core flow through the fuel channels. Both the reference 19 full/2 partial-LEU-core, and higher-element cores were modeled. Higher-element cores were examined to determine how the core flow distribution would change from adding additional elements to the LEU core. This would be done in the future to compensate for fuel burnup, as well as for other considerations.

5.2.2 19 Full/2 Partial-Element-Reference-LEU-Core

The reference LEU configuration was the first core modeled using PLTEMP. This subsection describes the key input parameters used in the development of the full-core model.

Several correlation indicators needed to be selected at the start of the code input. The heat transfer correlation (Sieder-Tate), the boiling correlation (Bergles-Rohsenow),

and the critical heat flux (CHF) correlation (Mirshak-Durant-Towell) were the default correlations selected. Two different types of fuel elements were chosen, corresponding to the difference in fuel loading between the full- and partial-LEU fuel elements. Three different flow bypasses were modeled, reflecting the difference in flow channel areas around the control blades, regulating rod, and radiation baskets. Graphite reflectors, having no flow associated with them, were not modeled as flow bypasses. Twenty different pressure drop increments were selected at which temperature and flow calculations were performed. Axial temperature distributions were not selected as output, as the full-core model was used primarily to determine the flow distribution, with downward selected as the direction of flow.

The 19 full-LEU elements were modeled first, and were split up into three axial regions, forming the inlet plenum, fuel region, and outlet plenum. A flow rate in kilograms per second had to be input as an initial guess, so a default value of 1 kg/s was used for all regions of the core. The hot channel factors used were the same as NATCON: 1.24, 1.25, and 1.35 for flow rate, heat flux, and heat transfer coefficient uncertainties, respectively.

Nineteen coolant channels were modeled to represent the areas between the 16 fuel plates and 2 end plates, and the areas outside the end plates. The fuel itself was modeled as U_3Si_2 -Al with the clad modeled as type-6061 aluminum. The fuel loading in the partial elements was one-half that of a full fuel element, although the fuel density stayed the same. This then corresponded to a reduction in the thickness of the fuel meat region in the fuel plates of the partial elements, with a corresponding increase in the cladding thickness. The widths of the water gaps were the same as the full fuel elements.

The flow bypasses were modeled next, starting with the five radiation baskets including the source holder and flux trap. Only one region was modeled for the radiation baskets. The flow area of the four control blades was modeled in a similar fashion as the radiation baskets, except the axial dimension was split into three separate regions representing above, around, and below the blades. The final flow bypass modeled was the regulating rod. It was split up into three regions representing above, around, and below the rod.

5.2.3 Higher-Element LEU Cores

As the core at the UMLRR undergoes operations, the uranium fuel in the elements will be slowly consumed, with fission products being built up in the fuel plates. Eventually the core will no longer be able to sustain criticality due to the fuel burnup and fission product buildup. Additional full elements were shipped with the LEU core, and currently reside in storage racks along the sides of the bulk pool. These elements will slowly be added to the LEU core to extend its lifetime. Therefore, additional full-core models in PLTEMP were created to see how the flow distribution in the core was affected by the addition of these new elements. These models consisted of 24 and 26 full elements. Graphite reflectors, having no flow associated with them, would be removed from the core grid to allow for the addition of these new elements. Hence, the only

changes to the input files were an increase in the number of full elements and a removal of the partial elements. Additionally, the effect of opening up one of the flooded, capped water baskets in the LEU 19 full/2 partial-element-reference-core was examined, as well as an 18-element core to see the alternate perspective of less elements. One radiation basket was unplugged to see how much the percentage of flow through the assemblies was affected, so that data on this case were available in case it was deemed there were not enough sample holders in the core.

5.2.4 Hot Channel Model

Once the flow distribution of the full core model of the reference LEU core was known, the hot channel model could be initiated. Only the hottest coolant channel of the hottest fuel element needed to be modeled to determine the power level where ONB would occur, as all of the other coolant channels would be below ONB conditions by default. The hot channel model input file was much more streamlined than the full model case, as only the physical data from one full fuel element, with no bypasses, was considered. Axial temperature distributions were calculated in this case. The same normalized axial distribution for the hot channel used in NATCON was also used in the PLTEMP hot channel analysis, with a corresponding axial peaking factor of 1.37. A radial peaking factor of 1.36 was used for each fuel plate in the assembly, since detailed intra-assembly power profiles were not available from the physics calculations. Applying the global radial peaking factor converts the average element into the peak or hot element.

Since there is no way to manually-input the coolant velocity in the PLTEMP input files, many different pressure drop increment cases were run until the pressure where ONB occurred was bracketed. This resulted in a pressure, and corresponding coolant velocity, above and below the point of ONB occurring somewhere in the hot channel for a given power level. The assembly power level itself was input as 5% of the total core power, corresponding to the analysis of one element in an effective 20 full element core. The two partial elements counted as one full element only for this case of average power produced per element.

5.3 PLTEMP CODE RESULTS

The results of the PLTEMP analysis are divided into two subsections. The full-core model results include the flow rate distribution for the reference 19 full/2 partial-element LEU core, as well as the higher element LEU cores. Hot channel analysis results include the development of a power-to-flow map, profiles of the burnout heat ratios, and various temperature profiles for the nominal 2-MW case at full flow.

5.3.1 Full-Core Model (Pump Flow Distribution) Results

The most important data gathered from all of the full-core models were the coolant flow rates through each element and bypass. From this information, the total core flow rate could be determined by adding up all of the flow rates through each individual region. This then allowed a calculation of the percentage of flow through only the fuel element to be determined. A criterion of approximately 70% was deemed an acceptable flow percentage through the fuel region.¹⁴

The flow rate through each full element was determined to be 4.13 kg/s, with the partial elements being slightly lower at 4.12 kg/s. The flow rate through the radiation baskets was 3.72 kg/s, the control blades 3.52 kg/s, and the regulating rod 1.65 kg/s. The total flow rate through the entire core was then calculated as 121.1 kg/s, setting the percentage of flow through the fuel region at 71.6%. Comparing to previous UMLRR core designs, the HEU core had a total flow percentage through the fuel region of 71.8%, and the value for the original 20-element LEU core design was 70.3%. Hot channel factors and power level changes had little or no effect on the results, as much of the calculation reduced to strictly a flow area geometry problem. A summary of the results for the reference LEU core is shown in Table 5.1.

As expected, the percentage of coolant flow through the fuel region increased when additional elements were added. This was done to simulate the effects of adding additional elements to the LEU core to compensate for fuel burnup and fission product buildup. Other scenarios studied included an 18-element LEU core, as well as the effect of uncapping one of the flooded and capped radiation baskets to increase in-core sample locations in the reference LEU core. A summary of the percentage of flow through the fuel region for all of the models is shown in Table 5.2. The results of this analysis show that the LEU cores have very comparable flow rates to the old HEU core. This was expected since the low areas were not changed significantly.

In order to analyze the effects of varying the number of elements in the core, a flow-to-power parameter was computed. This parameter represents the average core flow rate in kg/s per MW of power produced. The result of this analysis is shown in Table 5.2. For a higher flow-to-power ratio, more coolant is available to carry away the energy generated within the fuel elements. From the analysis, the higher-element 2-MW LEU cores have a higher flow-to-power ratio. As the UMLRR LEU core ages, additional assemblies will need to be added to counter fuel burnup. This proves that any addition of fuel elements to the 2-MW UMLRR LEU core will be conservative with respect to thermal hydraulic processes. Thus, a detailed analysis of the reference 21-element 2-MW core will be sufficient for characterization of all future configurations.

TABLE 5.1: PLTEMP REFERENCE LEU CORE FLOW RESULTS

Full Core PLTEMP Model
Parameters: Critical Case (Blades at 16.5 ")
Includes Hot Channel Factors, Power = 2 MW
of Full Elements = 19
of Partial Elements = 2
of Control Blades = 4
of Regulating Blades = 1
Total Flow Rate through the Core = 121.07 kg/s
Flow Area per Element = $5.6921 \times 10^{-3} \text{ m}^2$
Flow Area per Radiation Basket = $2.6391 \times 10^{-3} \text{ m}^2$
Flow Area per Control Rod = $8.9368 \times 10^{-3} \text{ m}^2$
Flow Area for the Regulating Rod = $6.4151 \times 10^{-3} \text{ m}^2$
5 Radiation Baskets (Including Flux Trap and Source)
Flow through each Full Fuel Element = 4.13 kg/s
Flow through each Partial Fuel Element = 4.12 kg/s
Flow through each Radiation Basket = 3.72 kg/s
Flow through each Control Blade Region = 3.52 kg/s
Flow through the Regulating Blade Region = 1.65 kg/s
Total Flow through all Full Fuel Elements = 78.47 kg/s
Total Flow through both Partial Fuel Elements = 8.24 kg/s
Total Flow through all Fuel Elements = 86.71 kg/s
Percentage of Flow through all Fuel Elements = 71.6%
Average Percentage of Flow per Fuel Element = 3.41%

TABLE 5.2: PLTEMP FLOW THROUGH FUEL REGION RESULTS

PLTEMP Flow Through Fuel Region Results	Core Power MW	Total Core Flow %	Assembly Flow Rate kg/s	Flow to Power Ratio kg/s per MW
UMLRR Core Configuration				
26 Element HEU Core	1	71.8	3.40	88
20 Element LEU Core	1	70.3	4.24	84
20 Element LEU Core	2	70.3	4.24	42
Reference 19/2 LEU Core	1	71.6	4.13	86
Reference 19/2 LEU Core	2	71.6	4.13	43
Reference 19/2 LEU Core (extra rad basket)	2	69.5	4.01	42
18 Element LEU Core	2	68.5	4.61	42
24 Element LEU Core	2	74.1	3.74	45
26 Element LEU Core	2	75.6	3.52	46

5.3.2 Hot Channel Analysis Results

The most important results of the hot channel analysis included the development of a power-to-flow map, a profile of the burnout heat ratios, and various axial temperature distribution profiles. The goal of the development of the power-to-flow map was to define the steady-state operating envelope of the UMLRR. A given power level was input into the PLTEMP code, and by narrowing in on the pressure change, the flow rate just above and below where ONB occurs at the given power level can be determined. The flow rate just below ONB was then used to set the flow envelope criterion. By running this scenario at different power levels, a curve can be generated for power-versus-flow rate, above which ONB will occur. This sets the minimum pump flow rate for the UMLRR at a given power level to prevent ONB. This analysis was done both with and without hot channel factors, and for several power levels ranging from 600 kW to 6 MW. For example, for a power level of 2 MW, ONB occurs somewhere between a flow rate of 702 to 707 gpm. The results of these analyses are shown in Table 5.3.

TABLE 5.3: PLTEMP HOT CHANNEL RESULTS

PLTEMP Results					
Thermal Analysis Results for Reference LEU Core					
With Hot Channel Factors					
Thermal Power	Flow Rate Below ONB		Flow Rate Above ONB		Burnout Ratio CHF/ONB Heat Flux
MW	kg/s	gal/min	kg/s	gal/min	
0.6	0.366	177	0.362	175	33
1	0.653	316	0.651	315	20
2	1.46	707	1.45	702	11
3	2.33	1128	2.32	1124	7.2
4	3.247	1573	3.246	1572	5.6
5	4.2112	2040	4.2106	2039	4.6
6	5.2089	2523	5.2086	2522	3.9
Without Hot Channel Factors					
Thermal Power	Flow Rate Below ONB		Flow Rate Above ONB		Burnout Ratio CHF/ONB Heat Flux
MW	kg/s	gal/min	kg/s	gal/min	
0.6	0.224	109	0.223	108	39
1	0.396	192	0.395	191	24
2	0.861	417	0.86	416	13
3	1.37	663	1.36	659	8.6
4	1.89	915	1.88	910	6.6
5	2.44	1182	2.43	1177	5.4
6	3	1453	2.99	1448	4.6

The desired power-to-flow map was derived from the results of Table 5.3. The power-to-flow map defines the steady-state operating envelope for the reactor wherein a combination of power and flow must be below the hot channel line on the graph to ensure a safe margin to ONB during steady-state conditions. The power-to-flow map, both with and without hot channel factors, is shown in Figure 5.1.

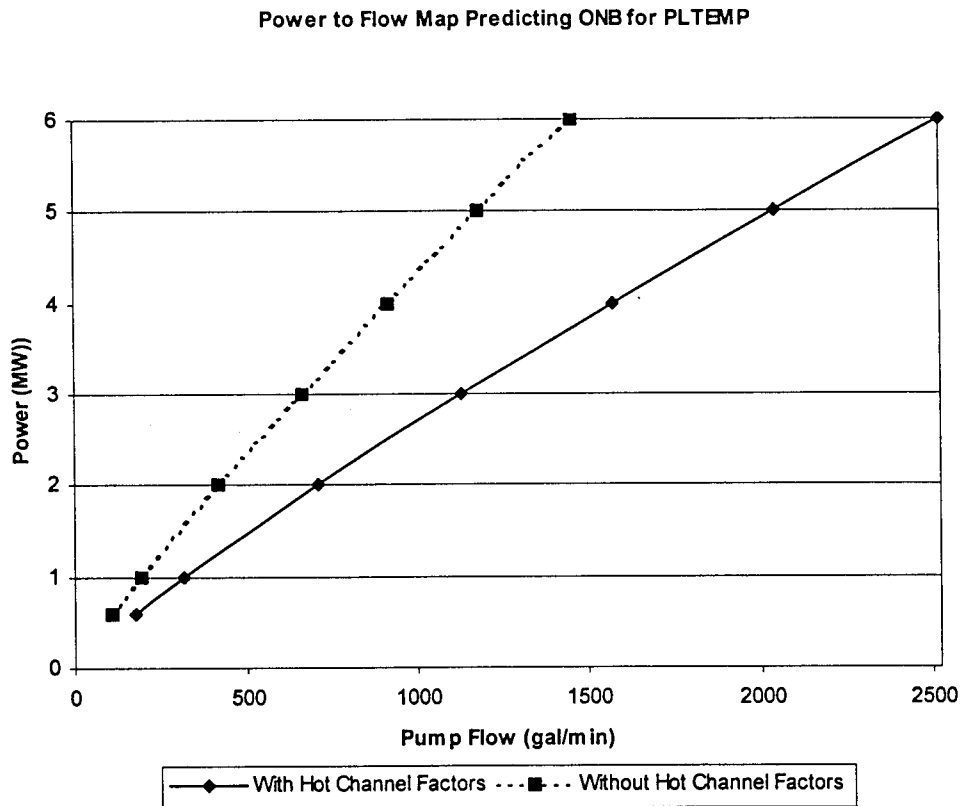


FIGURE 5.1: PLTEMP POWER-TO-FLOW MAP

The onset of nucleate boiling (ONB) refers to the initiation of the formation of microscopic vapor bubbles on the crevices of solid materials. The bubbles eventually detach when they grow large enough for buoyancy forces to overcome surface tension. The bubbles are then swept away by the coolant. When the bubbles become very large and detach quickly, full-blown nucleate boiling is occurring. Eventually, with increasing heat flux, the bubbles become so large that they begin to overlap each other and form a vapor surface on the solid material. This film boiling is also known as the departure from nucleate boiling (DNB). The heat flux at which DNB occurs is called the critical heat flux (CHF), also known as the burnout heat flux. At DNB, the fuel temperature starts to rise dramatically due to the vapor film having a much poorer heat transfer coefficient than the liquid. Eventually, fuel failure will occur as the temperature increases.

The ONB is the criterion for determining the safety limit of the UMLRR. The ratio of the critical or burnout heat flux (q''_c) to the heat flux at the ONB in the hot channel (q''_{ONB}) is called the burnout ratio. The critical or burnout heat flux can be computed using the following Mirshank-Durant-Towell correlation evaluated at the exit of the hot channel.

$$q''_c = 1.51 (1 + 0.1198 U) (1 + 0.00914 \Delta T_{sub\ exit}) (1 + 0.19 P)$$

q''_c = critical or burnout heat flux (W/m^2)

U = coolant velocity (m/s)

P = pressure (bars)

$$\Delta T_{sub\ exit} = (T_{sat\ exit} - T_{bulk\ exit}) (^{\circ}C)$$

At the exit of the channel, the coolant temperature will be at a maximum and, therefore, q''_c will be at a minimum. The burnout ratio represents the factor by which the heat flux at ONB would have to be raised in order to reach the DNB point that could cause fuel plate failure (cladding rupture). Since ONB is used as the safety criterion, this adds another built-in safety factor to the model. For example, at a power level of 2 MW, including the effects of hot channel factors, the heat flux that occurs at ONB would have to rise by over a factor of 10 before the critical heat flux is reached. The burnout ratios are included with the PLTEMP summary results in Table 5.3. The burnout ratios for the cases with and without channel factors, for several different power levels, are also shown graphically in Figure 5.2.

The final part of the forced-convection steady-state analysis was to examine how the temperature of the fuel, cladding, and coolant varied axially as flow progressed through the core. These data were obtained from the hot channel analysis at several power levels, both with and without hot channel factors, at a flow rate of 2,000 gpm. The key results for the nominal 2-MW case are displayed in Figures 5.3 and 5.4. The general trend of the fuel and cladding temperatures for all cases was to follow the hot channel axial flux profile, coming to a maximum about two-thirds of the way along the channel. Recall that the flux/power distribution is slightly bottom-peaked and that flow in the forced-convection cases is from the top (inlet) to the bottom (outlet) of the core.

In general, there was less than a one-degree Celsius difference between the fuel and cladding temperatures along the entire length of the fuel plate. This is due to the fact that the fuel plate is very thin. The coolant temperature increased fairly steadily in all cases. The differences for the cases with and without hot channel factors were significant. For example, for the 2-MW, 2,000-gpm case, in comparing with and without hot channel factors, the peak fuel and cladding temperatures differed by approximately 13° C, while the peak coolant temperature varied by about 2° C. With hot channel factors, the maximum cladding temperature for the 2-MW/2,000-gpm case was less than 80° C.

This is significant due to the fact that ONB does not occur during steady-state conditions until a clad surface temperature of approximately 120° C is reached. Thus, there is a significant safety margin at 2-MW operations.

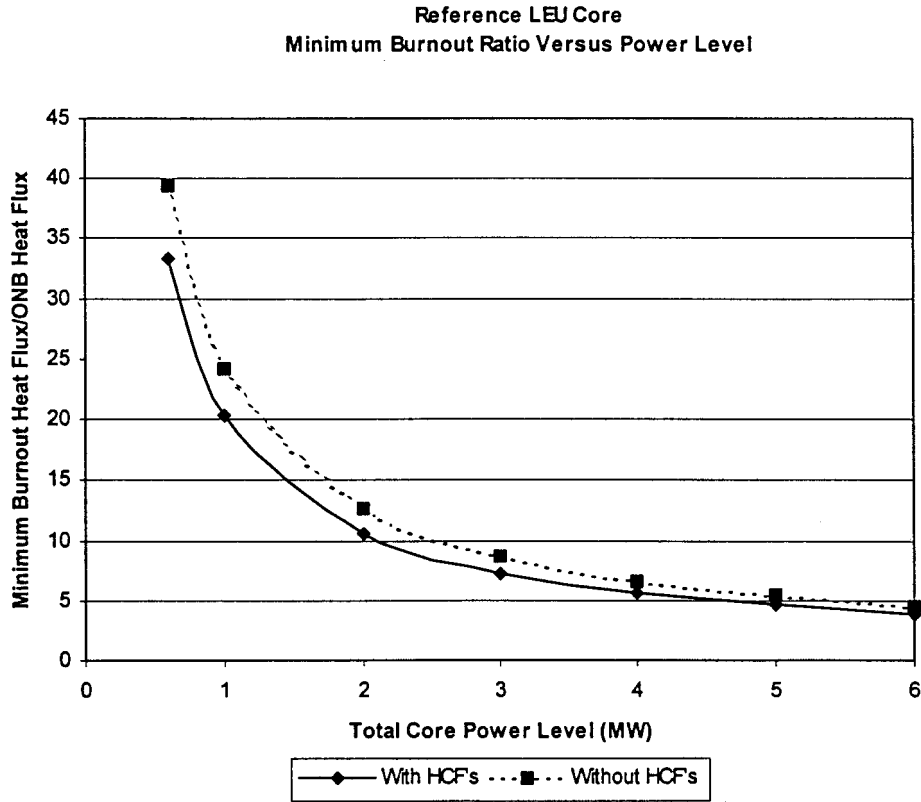


FIGURE 5.2: BURNOUT HEAT RATIOS

Note that the case with hot channel factors does not represent expected behavior during normal operations: it represents a worst-case scenario. The expected best-estimate behavior is represented by the curves in Figure 5.4 that do not include the hot channel factor uncertainties. These results, with and without hot channel factors, clearly show that the UMLRR can be operated safely during steady-state operations at 2 MW with a 2,000-gpm flow rate.

Note also that the temperature profile shapes were slightly different than the 200-kW natural-convection temperature profiles shown in Figures 5.3 and 5.4. This is attributed to the reversal of the direction of flow: upflow for natural convection versus downflow for forced convection, as the axial flux profile is bottom-peaked. In general, the magnitudes of the steady-state forced-convection temperatures at 2 MW are lower than the steady-state natural-convection temperatures at 200 kW. The flow-to-power rate for the 2-MW forced-convection core was 43 kg/s per MW, and for the 200-kW natural-convection core it was 20 kg/s per MW. This explains the higher natural-convection temperature profiles.

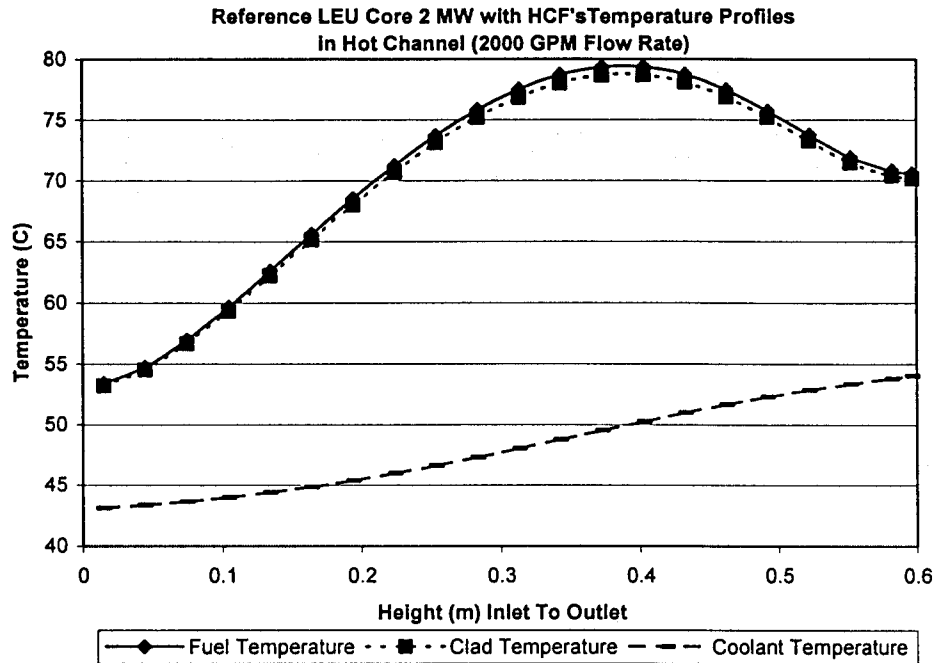


FIGURE 5.3: 2-MW TEMPERATURE PROFILES (WITH HOT CHANNEL FACTORS)

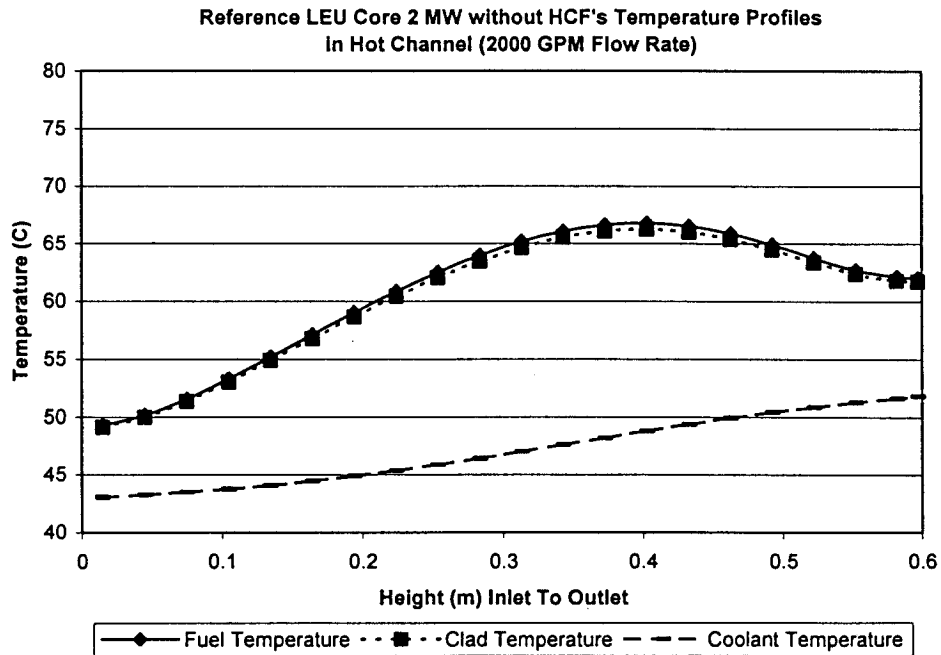


FIGURE 5.4: 2-MW TEMPERATURE PROFILES (WITHOUT HOT CHANNEL FACTORS)

6.0 TRANSIENT ANALYSIS

The previous sections dealt with the steady-state analyses for the reference LEU core. The intent was to define the power-to-flow envelope (Figure 5.1) for safe operation of the ULMRR under steady-state conditions and to quantify the expected nominal conditions at steady-state operation. However, the steady-state power-to-flow curve just sets an upper limit for the real operating regime of the reactor if no off-normal events were ever to occur. In practice, of course, a transient analysis needs to be performed to determine if the reactor can be operated safely under all conceivable transient scenarios. It is this transient analysis that sets the real operating limits for the reactor.

Typical research reactor accidents are generally defined under two broad categories: reactivity accidents and loss-of-flow accidents. Reactivity accidents occur when the reactor becomes inadvertently supercritical after operating at some steady-state power level. These reactivity transients result in increased transient power levels that exceed the designed steady-state power level. Loss-of-flow accidents can occur due to the complete or partial loss of pumping power. Temperature increases in the fuel and structural material of the core occur due to the increased heat production that occurs with both these accident scenarios.

Reactivity and flow transient calculations performed using the PARET-ANL code are described in this section. There were three broad categories of transients that were studied: rapid reactivity insertions, ramp reactivity insertions, and loss-of-flow transients. Rapid reactivity insertion transients can occur due to operator error, or malfunction or failure of a reactor core component. Ramp reactivity insertion accidents can occur due to continuous withdrawal of a control blade during reactor startup. Loss-of-flow transients can occur due to pump failure. These analyses were performed in order to characterize the behavior of the UMLRR under transient conditions, and included a broad range of conditions over a variety of configurations.

6.1 PARET-ANL CODE DESCRIPTION

The PARET-ANL code allows for coupled point kinetics, hydrodynamics, and thermal capability. The entire reactor core can be described by up to four regions, which may have varying coolant mass flow rates, power generation, and other hydraulic parameters. These regions are broken down into single fuel plates centered within a coolant channel. The heat transfer in the fuel plates is modeled both radially and axially. The one-dimensional radial heat conduction model can consist of up to a total of 43 sections of fuel, clad, and gap. Up to 21 axial nodes can be used for the axial model. Coolant regimes can range from subcooled liquid to superheated steam, and heat transfer may be either natural or forced convection. Steam was not allowed to form in the coolant under the current UMLRR analysis, as the limiting case was the onset of nucleate boiling. PARET-ANL also allowed for flow reversal to occur under natural convection conditions. Externally specified reactivity may be specified as a function of time, and the axial power distributions may be specified for each of the core regions. The effects of

changes in moderator density and temperature, and fuel temperature and linear thermal expansion are taken into account by the total reactivity feedback. In each of the core regions, the respective coefficients may be specified. Each of the core regions may be subdivided into clad, gap, and fuel zones, up to a maximum of 43 radial sections. The PARET-ANL code includes an extensive library of coolant properties, particularly applicable to research reactors, including those occurring during low temperatures and pressures as compared to a power reactor. The code is described in detail in Reference 7.

6.2 PARET-ANL CODE MODEL (REFERENCE LEU CORE)

Described in this section are the general assumptions and models that were used in the input specifications for each configuration. A two-region (or two-channel) model was used in the PARET-ANL code. The entire core was divided into two regions with this mode. One region (or channel) represented the hottest fuel plate. The other region (or channel) represented the rest of the core. Over the active core region, the axial dimension for each channel was divided into 21 equally-spaced nodes. Within the clad and fuel regions, radial heat conduction was treated with 7 discrete nodes. Slab geometry was used since the reactor core of the UMLRR consists of plate-type fuel elements. A reactivity-specified operation mode was used in the reactivity transients, as opposed to a power-specified mode. This allowed the user to set the externally-inserted reactivity as a function of time during the transient. The power level of the reactor then changed based upon the reactivity inserted. In all cases, six delayed neutron groups were used. Appropriate to each configuration, the value of initial reactor power was specified in megawatts. The total volume of fuel in the reference LEU core was calculated from the meat and fuel dimensions in Reference 15. In all of the cases, the core inlet pressure was specified.

The inlet moderator temperature was used instead of the enthalpy of inlet moderator at the user's option. The code converts the temperature into the corresponding enthalpy and proceeds as usual when it reads a negative temperature value. The end sections of the fuel elements, which contain no active fuel, were taken as zero since only the active fuel regions were modeled. The effective delayed neutron generation time and the prompt neutron generation times were obtained from the UMLRR FSAR Supplement.¹

After several practice runs of each kind of transient calculation, a reasonable set of consistent transient time values were obtained. Typical values were 100 seconds for loss-of-flow transients, 6 seconds for ramp reactivity transients, and 0.6 seconds for step reactivity transients. At an inlet temperature of 43° C, the moderator reference density is 991.67 kg/m³. The PARET-ANL code allows for a fuel temperature feedback equation incorporating up to a fourth order polynomial in temperature, but a linear model was used.⁷ This is used to compute the reactivity feedback from fuel temperature changes, primarily from Doppler broadening. The UMLRR LEU uranium fuel consists of 80% of the ²³⁸U isotope. ²³⁸U absorbs neutrons, especially in the resonance energy region, and this affects the neutron balance in the core due to its relatively high absorption cross-sections. When the fuel temperature increases, ²³⁸U neutron absorption increases due to

resonance broadening in the center of the fuel. This leads to a negative feedback effect, which decreases reactor power. This phenomenon is known as Doppler broadening, and it reduces reactivity while increasing resonance absorption. The UMLRR LEU core has a relatively large negative Doppler reactivity coefficient, especially relative to the HEU core, which contributes significantly to the safety of the LEU-fueled reactor.

An optional voiding model for subcooled boiling is included in the PARET-ANL code. Depending upon the degree of subcooling, there are certain adjustable parameters that must be set by the user. These parameters do not affect the results for the current study, since the transients performed here do not extend to the subcooled boiling region, which is beyond ONB.¹⁶ However, these parameters are still needed in the calculations.

PARET-ANL can be used to perform transient calculations including single- and two-phase heat transfer correlations, departure from nucleate boiling, and flow instability. The Seider-Tate correlation was chosen for the single-phase heat transfer computations, and the Bergles-Rohsenow correlation was chosen for the two-phase heat transfer computations. These correlations were chosen so that they would be consistent with the choices that were made for the steady-state analyses using PLTEMP.

The overpower trippoint was set at 115% of the initial reactor power for the 200-kW natural-convection and 2-MW forced-convection cases. This represents the Limited Safety System Setting (LSSS) for an increased power level core. An alarm setpoint of 105%, a scram setpoint of 110%, and an LSSS of 115% are anticipated for operation of a 2-MW forced-convection core (and a corresponding 200-kW natural-convection core). These are tighter setpoints than are currently used, but are operationally practical and reasonable. Since the current analyses center around the concept of a single-failure criterion, the overpower trippoint is one of the key parameters of the reactivity transient analyses. The trippoint determines the exact time at which the control rods begin to drop. It also has a strong effect on the maximum power level reached for a given transient, with Doppler broadening being the other major contributor.

One of the most significant parameters for the loss-of-flow transients is the lowflow trippoint. The lowflow trippoint was set at 80% in all of the analyses. This value reflects current UMLRR criteria. The reactor scram is initiated when the pump flow is reduced to 80% of its initial value, in the event of low primary flow. A previous operating time of 48 hours was used; this reflects the approximate time it takes to come to Xenon equilibrium. This parameter is needed to compute the decay heat level after the scram. The power level of the reactor at the beginning of the transient was used as the previous operating power of the reactor, reflecting an equilibrium condition before the transient.

The control blade drop speed was determined by performing drop-time measurements. By electronically-cutting off the current through the electromagnets, therefore de-energizing them, the weight of the control blades will cause them to fall during a scram. The slowest control blade speed was determined to be 0.8 m/s, which was used as the default control blade speed in all of the transients. The scram delay time

was taken to be 280 milliseconds from the FSAR. Reactor scram initiation takes place but the control blades do not drop instantaneously in the event of an overpower or loss-of-flow trip setting. The control blade-worths were modeled by PARET-ANL as a single control blade by combining all of the reactivity from each of the four UMLRR control blades together at a given height.

The volumetric heat capacity and thermal conductivity models are defined by five coefficients each in PARET-ANL. In the UMLRR input models, thermal conductivity was assumed to be independent of temperature. For consistency, the thermal conductivity of the LEU fuel, which consists of a U_3Si_2 -Al ceramic, was obtained from PLTEMP. The volumetric heat capacity was assumed to vary linearly with temperature.

Due to the slab geometry of the fuel plates, the half-plate thickness of the fuel plate was needed. This represents the plate thickness from the outer surface of the clad to the centerline of the fuel. The number of radial points in the analysis was 7, consisting of 2 clad radial points and 5 fuel radial points. No gap was modeled between the fuel and the clad. The geometry of the fuel and the clad was described separately in the PARET-ANL input files.

In the PARET-ANL code, axial spacing in the active fuel region begins at the bottom and proceeds to the top. The fuel region was divided into 21 axial mesh regions. At the bottom of the fuel, the first mesh node point is situated. Similarly, the last mesh point is located at the top of the fuel. All of the other mesh points are located at the centers of their axial regions. The volume of the fuel associated with the first and last meshes is half of all the other meshes. This requires the thickness of the first and last mesh to be half that of the other meshes. This allowed the 21 axial node points to be placed at equal distances from each other, with each distance representing 1/20 of the active length of the fuel element. Therefore the same axial profile as PLTEMP was used, but with the axial profile inverted in the input file. The geometry requirements of the PARET-ANL code require that the axial profile be described from the bottom of the core to the top. This means for forced-convection flow, top-to-bottom, this is in the opposite direction than the modeling requirements of PLTEMP, which require an inlet-to-outlet axial description. Since in forced-convection flow the inlet of the core is at the top, PLTEMP and PARET-ANL have opposite axial profiles. In natural-convection flow, bottom-to-top, PARET-ANL and NATCON axial profiles agree, as NATCON uses an inlet-to-outlet criteria for its axial profile.

In the transient analysis, the core was divided into two sections consisting of a hot channel and the rest of the core. The remainder of the core was considered an average channel. For the reactivity transients, the core mass flow rate needed to be specified initially. For the loss-of-flow transients, the core mass flow is represented as a function of time through a pump coast-down curve.

Several other channel parameters were needed. The radial distance from the center of the water channel to the center of the fuel was required. The reactivity feedback weighting factor for each channel was also needed. For the hot channel, this represents

the ratio of the volume of fuel in one fuel plate to the total volume of fuel in the core. For the average channel, this was just unity minus the reactivity feedback weighting factor for the hot channel.

Due to the limitations of the PARET-ANL code, an accurate description of the inlet and outlet plenum regions could not be modeled. It was assumed that the plena were fully mixed in order to simplify the general solution procedure. This resulted in no need for analysis of the temperature and velocity fields in the plena. Another assumption made was that no transverse pressure gradients existed in either plenum. This allows for the pressure drops in all of the channels to be equal. Therefore, in the UMLRR model, the lengths of the inlet and outlet plenum regions were taken as zero and not modeled. This then allows the diameters of the inlet and outlet plenum regions to become insignificant, as they must be modeled as a positive value in the PARET-ANL code. Therefore, they were arbitrarily set to unity in the UMLRR model.

As previously mentioned, the fuel was divided into 21 axial regions. Since in the UMLRR analysis the core was divided into two regions, PARET-ANL requires the axial power profiles for each region. As mentioned previously, the axial profiles were described in the PARET-ANL input file from the bottom of the core to the top of the core. A radial peaking factor of approximately 1.4 was used to account for the power difference between the hot and average channels in the UMLRR core. Also needed for each region are the reactivity feedback weighting factors associated with coolant temperature, Doppler broadening, and moderator density. The axial source description, or power profile, incorporated in PARET-ANL was taken from in-house reactor physics computational models with the control blades at 16.5" withdrawn. This represents a bottom-peaked axial profile, and is considered to be a more conservative modeling approach than a traditional cosine shape with the control blades fully-withdrawn from the core. This is due to the bottom-peaked profile having a larger maximum than the cosine profile. Since the reactivity insertion rate has a major role in the safe shutdown of the reactor, it was decided to model the transient reactivity analyses with the control blades at a fully-withdrawn position. This added to the conservatism of using a bottom-peaked power profile, since very little reactivity-worth exists at the ends of the control blades. Subsequently, more time is needed for significant reactivity-worth to be inserted into the core. This allows for the shutdown of the reactor to occur later than if the reactor was operated with the control blades already partially in the core, thus adding additional conservatism to the model.

PARET-ANL provides for feedback from changes in the coolant with respect to temperature, density and voiding resulting from Doppler broadening and the expansion of the fuel plates with temperature. For each of the axial regions, separate weighting factors can be assigned for each of these major feedback mechanisms. Uniform axial weighting factors were assigned for all regions and for all coefficients due to the assumed uniform fuel loading. The product of the total reactivity coefficient and the respective weighting factor yields the value of the local reactivity coefficient at each node.

Delayed neutron information was required for the six delayed neutron groups since a reactivity-specified operational mode was used in the analysis. The two parameters that are required for each group are the delayed neutron fraction and the decay constant. ENDF/B-V data files were used to obtain the delayed neutron fractions and decay constants.

The reactivity that is externally-inserted with respect to time is given as a pair of entries in the PARET-ANL input files due to the adaptation of the reactivity specified problem. This is done for either a step reactivity insertion or a ramp reactivity insertion, and it is one of the most significant entries for performing the reactivity transient analyses. The default step change reactivity value was 0.50% $\Delta k/k$, representing the single failure criterion of one fixed sample of maximum reactivity instantaneously decoupling from the reactor core, although other reactivity values were examined as well.

The default ramp change reactivity value was 0.054% $\Delta k/k$ per second, representing the continuous withdrawal of the regulating rod at its Technical Specification reactivity limit. The reactivity of the control blades was specified in dollars (\$) and the time in seconds. The conversion to dollars was achieved by dividing the reactivity values by the effective delayed neutron fraction (β_{eff}), which is equal to 0.0078 for the UMLRR LEU core. PARET-ANL uses a linear interpolation scheme to determine the reactivity values in times between those given in the input file.

In the PARET-ANL input file, the moderator inlet mass velocity in the core versus time can also be specified. The default value for the forced-convection transient cases was a nominal pump flow rate of 2,000 gpm. In the input file, the mass velocity needed to be converted to a mass flux with units of kg/s/m^2 . The fraction of flow through the fuel region of the UMLRR core is approximately 72% from the PLTEMP full core flow analysis, and was used to find the value of the mass flux, being approximately $1,170 \text{ kg/s/m}^2$.

PARET-ANL provides for user-input of the time steps in which neutron kinetics calculations are carried out. This is useful since it allows for more time steps during the key time periods of interest in the transient, such as when the control blades drop into the core during the reactivity transients, and the time of flow reversal for the loss-of-flow transients. These times of interest varied depending on the transient scenario, and needed to be determined by running an initial case at an arbitrary time step. Computational time in general was not an issue in the limitations of small time steps, as the typical PARET-ANL code run took less than one minute to complete on a 500-MHz processor. However, the value of the total number of time steps used is required to be known in order to execute the post-processor routine. This routine is used to extract specific results of interest from the PARET-ANL output file. If zeroes are entered for the time steps, PARET-ANL attempts to calculate its own time steps. In general, this method was not preferred as the code tended to choose large time steps, thus reducing both the quantity and quality of output. Those time dependent profiles did not have enough resolution, and thus did not reveal much detail about the consequences of an accident for both reactivity insertion and loss-of-flow. Therefore, user-chosen time increments were preferred.

The quantity of major calculational results desired was also controllable by the user. The user can specify how many time steps elapse before calculational results are shown in the output file. The output file also contains a complete listing of the input information. The calculational results include the core power, elapsed reactor time, and reactivity feedback for each requested time step number. The reactivity feedback is broken down with respect to origin, such as Doppler broadening and rod expansion. The code output also includes burnout ratio, heat flux, mass flow rate, void fraction, specific volume, coolant enthalpy, and temperatures of the clad, fuel, and coolant at each axial node point of each channel.

The user also has control over certain other intermediate printouts such as total reactivity, reactor power, and the maximum temperature in the clad, fuel, and coolant, apart from the above mentioned detailed output edits. These intermediate printout temperatures represent volumetric average temperatures averaged radially across each axial section. In general, these intermediate printouts were not needed, as most of the data from PARET-ANL was extracted from the output file using the post-processing routine. The post-processing routine makes many of the key parameters versus time, including minimum critical heat flux, mass flow rate, reactivity, and power available in easy to use form. Also available are the coolant outlet, maximum clad surface, and maximum fuel centerline temperatures.

Due to the assumption of a single failure criterion in the case of reactivity transients, the pump flow remains constant through the transient. In other words, no loss-of-flow is assumed to occur during a reactivity transient. A pump coastdown was superimposed by specifying the pump mass velocity fraction versus time for the loss-of-flow transients. Loss-of-flow was modeled three different ways for the UMLRR core. An exponential flow loss was modeled with a time constant of approximately 8 seconds. A linear flow loss model was also used with zero flow occurring at approximately ten seconds. Real data from the UMLRR primary pump were also obtained during its coast down, although it was limited to the range of 100% to 50% of maximum flow due to instrumentation noise. Flow loss was also modeled using these data, with the pump assumed to stop completely at 50% of flow. This was denoted as the truncated case. The results of these cases are all discussed in detail in the next section.

The final parameters of the PARET-ANL input file require the total control rod-worth inserted in to the core versus distance of insertion. This was obtained by summing the total reactivity-worth of the four UMLRR control rods at each height step. Rod-worth was obtained from the UMLRR staff from their required annual Technical Specifications control rod-worth determination. In conjunction with the rate of control rod movement in the case of a scram or rod withdrawal, the values are used to yield the reactivity rate in $\$/\text{second}$. For blade insertion, PARET-ANL requires negative values of reactivity to be input. The total worth of the four control blades was determined to be approximately $\$15$. The UMLRR control blades are currently withdrawn approximately 15 inches from the reactor core under typical operating conditions. In the fully-withdrawn position, less reactivity is inserted during the beginning of the transient. The

power drop-off after the scram will then be slower, thus adding conservatism to the model. From a safety standpoint, the peak power reached before the scram is of importance in the reactivity transient analyses. The change in reactivity at the beginning and end positions of the control rods is minimal due to the low flux in these regions of the core. At the center of the core, where the flux is greatest, the change in reactivity is also the greatest.

6.3 PARET-ANL CODE RESULTS (REFERENCE LEU CORE)

The reactivity transient and loss-of-flow analyses were carried out after having generated several general input models with some conservative assumptions. Two kinds of reactivity transients were studied. Rapid reactivity insertions were studied in the form of step insertions, and slow reactivity insertions were studied in the form of ramp insertions. Step insertions model an in-core sample with high reactivity-worth instantaneously decoupling from the reactor core. Ramp insertions model accidental continual regulating rod withdrawal. Loss-of-flow transients were modeled three ways: using exponential, linear, and truncated pump coast-down models. These three scenarios model a loss of primary pump flow due to pump shutdown or blockage, and describe the behavior of the coolant flow rate as the pump coasts down during the transient. The following sections discuss the results obtained from the transient analyses.

6.3.1 Step Reactivity Insertion Results

The maximum power levels reached under various levels of step insertion of reactivity were modeled using the PARET-ANL code. This was done in order to establish that the conditions reached in a transient state were within the operating domain. The operating domain is bounded by the onset of nucleate boiling (ONB), regardless of the maximum power reached during the transient. As long as ONB was not reached during the transient, the safety conditions were met. Computational analyses of near instantaneous insertion of reactivity at many different power levels were carried out. The most important power levels studied were 200 kW and 2 MW. The reactor was assumed to be operated under forced convection at 2 MW, and under natural convection at 200 kW. These power levels represented the proposed new maximum power level limits of the UMLRR for forced- and natural-convection, respectively. The reactor behavior was also observed under many different levels of instantaneous insertion of reactivity. The most important reactivity insertion level studied was 0.5% $\Delta k/k$, which represents the single failure criterion of a Technical Specifications maximum-worth fixed sample instantaneously decoupling from the UMLRR reactor core. Various pump flow speeds were also used, up to 2,000 gpm. This represents the maximum rated flow rate of the existing primary pump.

The step reactivity insertions from an initial power level of 2 MW were assumed to occur under nominal pump flow conditions of 2,000 gpm. The case of a 0.5% $\Delta k/k$ instantaneous insertion of reactivity in the 2-MW LEU core is considered in the following discussion. The Limited Safety System Setting (LSSS) is anticipated to be set at 115% as discussed previously.

Consequently, in a 2-MW core, a trip setting was set for 2.3 MW. In addition, the control rods do not begin to drop into the core until after a delay of 280 milliseconds from the initiation of the scram. The results of this analysis are shown in Figure 6.1. The transient analysis followed the effects of the prompt jump, the scram initiation due to the reactor trip setting, the delay time involved in the reactor scram, and the subsequent effect on the power of the control blades dropping into the core. The maximum power occurred at about 5.5 MW. The most interesting result of this analysis was the fact that the peak power level occurred before the control blades even started to drop into the reactor core. This was due to the large negative Doppler coefficient of reactivity associated with the LEU core. This Doppler broadening effect adds a significant amount of safety to the UMLRR core.

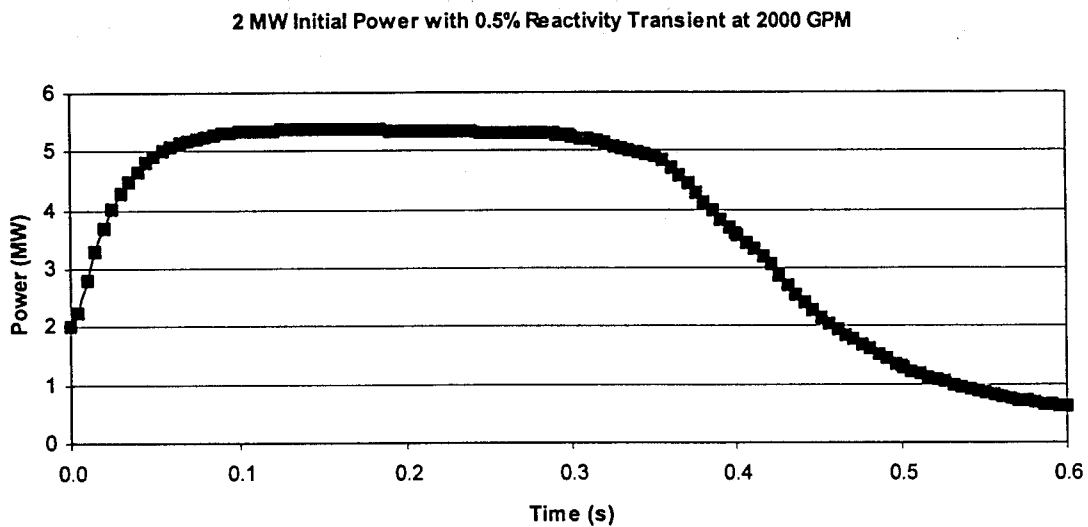


FIGURE 6.1: 2-MW STEP-CHANGE REACTIVITY TRANSIENT POWER PROFILE

The peak hot channel cladding temperature during the transient is shown in Figure 6.2. Due to the thinness of the fuel plates, the peak fuel and cladding temperatures differ by less than one degree, so fuel temperature was not plotted. The maximum temperature attained is approximately 90° C. The most interesting result is that the temperature peaks after the control blades have already started to fall. During the analysis, it was determined that ONB does not occur until at least a clad temperature of 120° C. The margin of approximately 30° C until ONB is reached, combined with the effects of Doppler broadening, ensures the safety of the reactor.

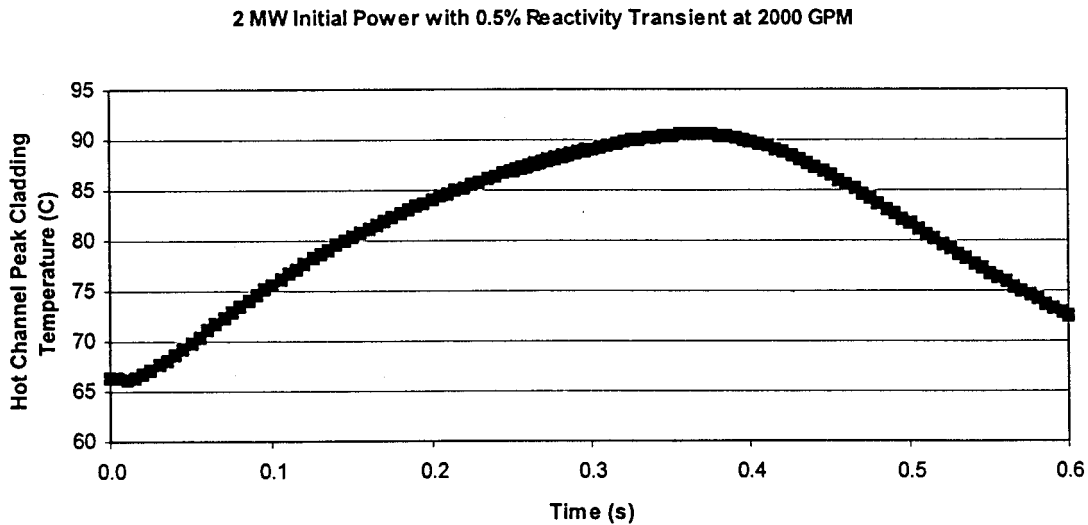


FIGURE 6.2: 2-MW STEP-CHANGE HOT CHANNEL PEAK CLADDING TEMPERATURE PROFILE

A step reactivity insertion from an initial power level of 200 kW was also assumed to occur under natural convection. The results obtained for a 0.5% $\Delta k/k$ instantaneous insertion of reactivity are indicated in Figure 6.3. The natural convection overpower trippoint was set to 230 kW, 115% above the initial power of 200 kW for the same reasons as the forced-convection argument mentioned previously. In this case there is no pump flow, and the initial mass velocity was obtained from the NATCON code output using the fixed power level option for 200 kW. The core mass velocity was calculated from NATCON for the case without hot channel factors, as PARET-ANL does not have the capability to model them explicitly.

The same axial flux profile that was used in NATCON and PLTEMP was also used in PARET-ANL. Since PARET-ANL always models its axial profile from bottom to top, rather than inlet to outlet, there was no need to reverse the profile when switching from natural- to forced-convection, as had been done with comparing NATCON to PLTEMP. In PARET-ANL, there are gravity and flow direction flags to indicate the orientation of the reactor and flow. The core mass velocity under these natural-convection conditions at 200 kW was approximately 55 kg/s/m^2 in the UMLRR LEU core. The 200-kW transient analysis for this case showed similar effects to the 2-MW transients, with the prompt jump, reactor trip (at 230 kW), scram initiation, and eventually the rapid power drop due to the control blades dropping in to the core. It can be observed that the LEU core peaks at about 620 kW. Results similar to the forced-convection analysis were seen. The peak hot channel cladding temperature during the transient is shown in Figure 6.4. The maximum temperature attained is approximately 65°C , which is reached after the control blades have already started to fall. Again, since the margin to ONB is still approximately 55°C , the reactor is clearly safe for this worst-case transient condition for the 200-kW natural-convection reference steady-state power level.

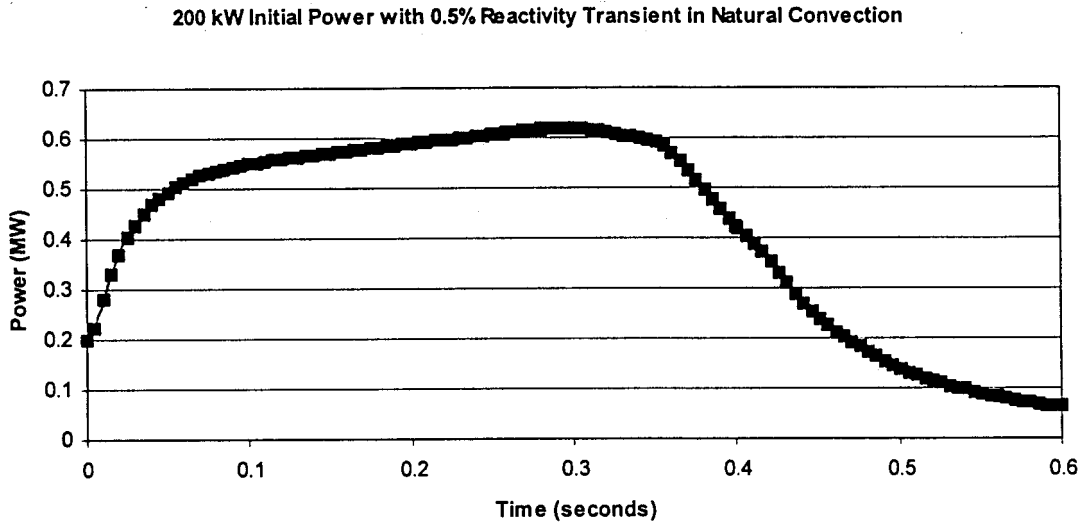


FIGURE 6.3: 200-KW STEP-CHANGE REACTIVITY TRANSIENT POWER PROFILE

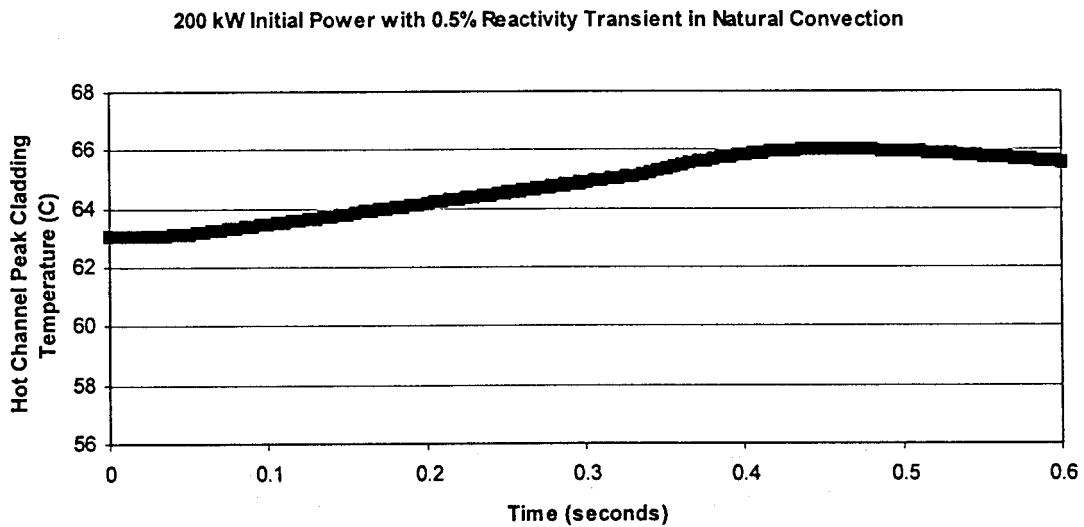


FIGURE 6.4: 200-KW STEP-CHANGE HOT CHANNEL PEAK CLADDING TEMPERATURE PROFILE

6.3.2 Ramp Reactivity Insertion Results

In this part of the analysis, the consequences of the continuous withdrawal of the regulating rod with an initial power of 2 MW and a flow rate of 2,000 gpm was investigated. The current UMLRR Technical Specifications state that the limit of the rate of reactivity insertion for the regulating rod is 0.054% $\Delta k/k$ per second. This is a more limiting case than the control blade rate of reactivity insertion. Even though the UMLRR control blades are each worth approximately 10 times the worth of the regulating rod based upon the blade-worth curves, the control blades have a much slower rate of withdrawal. Therefore, the regulating rod is seen as the limiting case. The analysis was performed assuming that the reactivity was added at a continuous rate of 0.054% $\Delta k/k$ per second. The results obtained for this 0.054% $\Delta k/k$ per second ramp insertion rate of reactivity are indicated in Figure 6.5.

The UMLRR LEU core power level was observed to peak at about 2.4 MW. The peak hot channel cladding temperature during the transient is shown in Figure 6.6. The maximum temperature attained was approximately 70° C. This was much lower than the step change maximum temperature of 90° C. Again since ONB is the limiting safety factor, and not the peak temperature attained during the transient, the reactor is still safe under these conditions. The bottom line of this analysis is that the ramp insertion of reactivity is a less limiting condition than the cases involving an instantaneous insertion of reactivity.

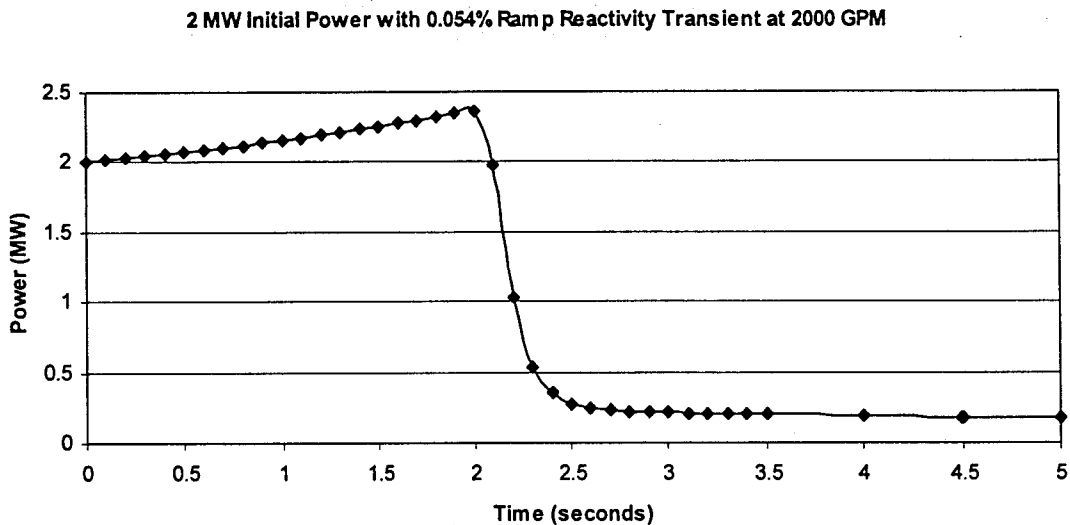


FIGURE 6.5: 2-MW RAMP REACTIVITY TRANSIENT POWER PROFILE

2 MW Initial Power with 0.054% Ramp Reactivity Transient at 2000 GPM

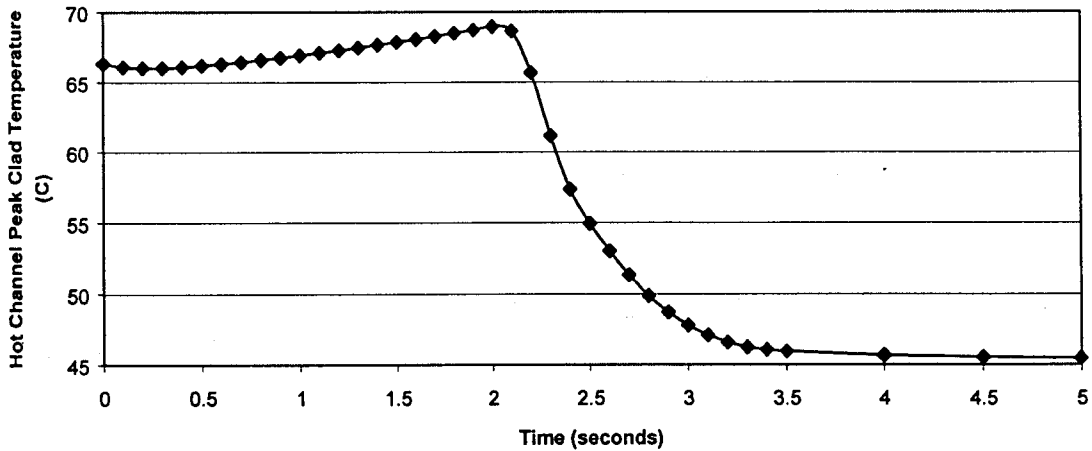


FIGURE 6.6: 2-MW RAMP HOT CHANNEL PEAK CLADDING TEMPERATURE PROFILE

6.3.3 Loss-of-Pump-Flow Results

If pumping power is ever lost during operation of the UMLRR, decay heat is ultimately removed by natural convection in the upward direction. This means that flow reversal will ultimately occur during the transition from forced- to natural-convection. However, a period of very low flow will occur before the flow inversion. The intent of this analysis was to perform the required computations that could give an estimate of the peak clad temperatures under loss-of-flow conditions. PARET-ANL also predicts the flow inversion process after pump failure.

Three different models were used to simulate the loss of flow. These models were termed the truncated, exponential, and linear flow loss scenarios. The history of the UMLRR primary pump coastdown could be measured with the reactor instrumentation. However, due to instrumentation limitations, the flow coastdown could not be measured accurately below 50% flow. Therefore, one loss-of-flow model consisted of using the measured data up to 50% flow, and then having the pump flow below 50% equal to zero. This was called the truncated model. The experimental flow rate data were also fit to exponential and linear curves. These curve fits made up the other two models. The exponential model was assumed to decay exponentially with a time constant of approximately 8 seconds. The pump time constant is the time it takes for the flow to fall to 1/e of its maximum value. The linear model had pump flow terminate at approximately 10 seconds. These three models are compared in Figure 6.7 for the range of 100% to 50% flow. The indicated data have been normalized to an initial nominal flow rate of 2,000 gpm. PARET-ANL allows the user to specify these values in any desired time history. In the exponential model, it is difficult to show exactly when the pump head goes to zero. After 70 seconds, the flow rate had reduced to less than 1/100 of 1% in the exponential model, and that was considered to be zero flow.

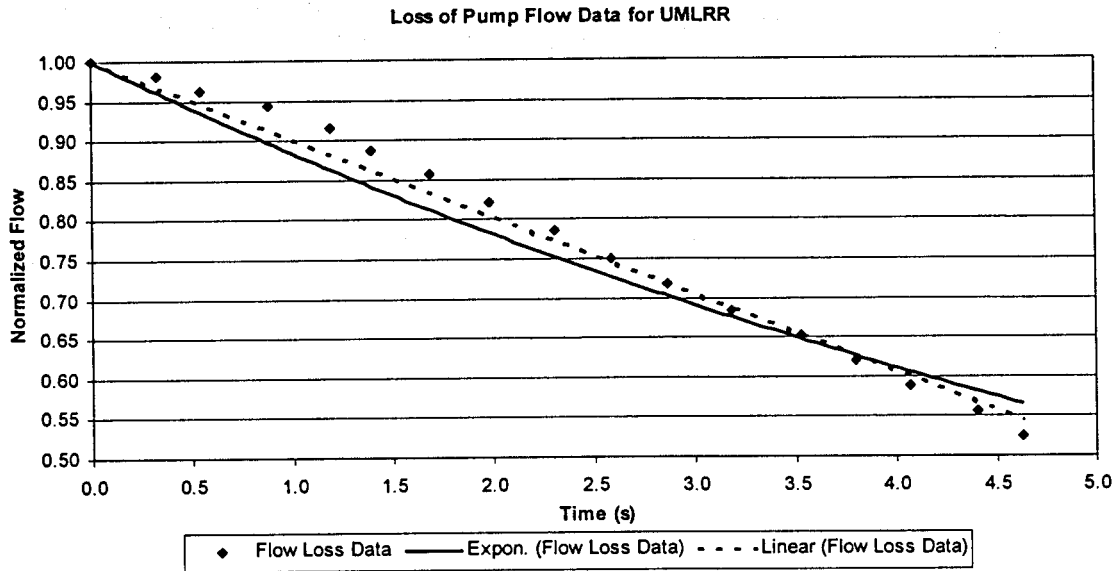


FIGURE 6.7: COMPARISON OF TRUNCATED, EXPONENTIAL, AND LINEAR FLOW LOSS

Current UMLRR LSSS criteria state that in the event of a loss of primary flow, the reactor will scram when the flow reaches 80% of the initial rated value. The loss-of-flow analysis was performed at the 2-MW power level and a 2,000-gpm flow rate for the UMLRR LEU core. Figure 6.8 shows the mass flux profile obtained from the loss-of-flow analysis for the truncated flow case. The initial mass flux of approximately $1,170 \text{ kg/s/m}^2$ corresponds to the nominal flow rate of 2,000 gpm. The mass flux is initially negative due to downflow being represented as negative in PARET-ANL. The flow reversal occurs at approximately 10 seconds into the transient. Figure 6.9 shows the temperature profiles associated with the truncated case. One of the main points of interest in this analysis was to observe the peak cladding temperature under reduced flow conditions. As shown in Figure 6.9, the maximum cladding temperature in the hot channel is approximately 70°C . The maximum cladding temperature is experienced during the initial stages of the transient, just after the reactor scram. At this stage, the power produced at a level of 2 MW, under drastically reduced flow conditions, resulted in a high rate of heat production and a low rate of heat transfer. Since ONB occurs at a cladding temperature of approximately 120°C , there is a significant margin to ONB. The hot channel cladding temperatures around the flow reversal time also do not exceed the initial maximum, so the truncated model is not seen as a limiting case.

Figure 6.10 shows the mass flux profile obtained from the loss-of flow-analysis for the linear flow case. The flow reversal also occurs at approximately 10 seconds into the transient. Figure 6.11 shows the temperature profiles associated with the linear case. The maximum cladding temperature in the hot channel also was approximately 70°C , and also occurs shortly after the reactor scram. The hot channel cladding temperatures

around the flow reversal time also do not exceed the initial maximum, so the linear model is also not seen as a limiting case.

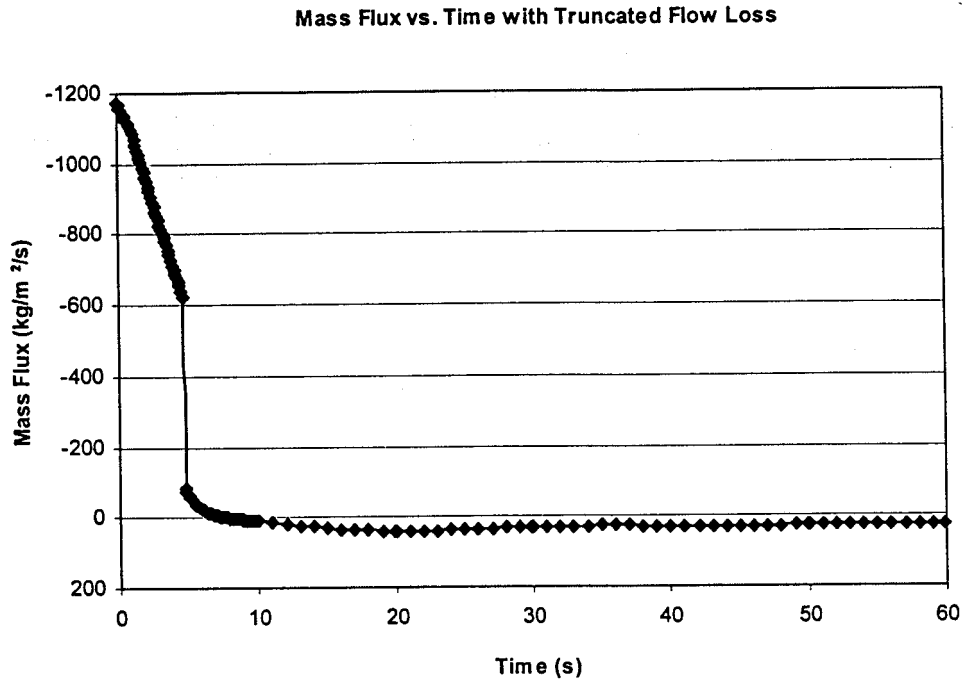


FIGURE 6.8: TRUNCATED MASS FLUX PROFILE

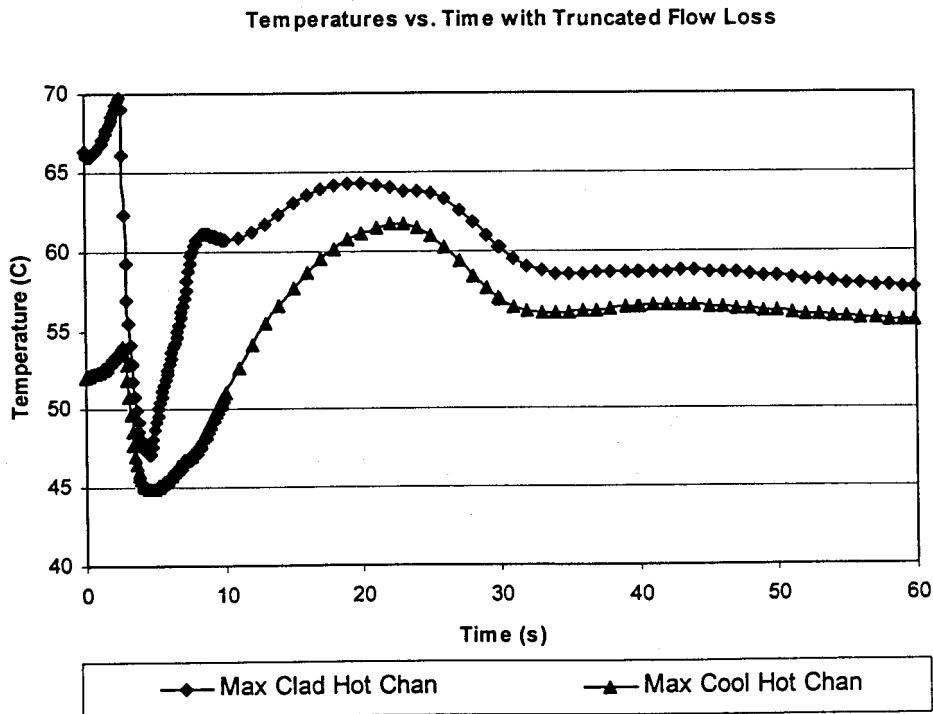


FIGURE 6.9: TRUNCATED TEMPERATURE PROFILE

Mass Flux vs. Time with Linear Flow Loss

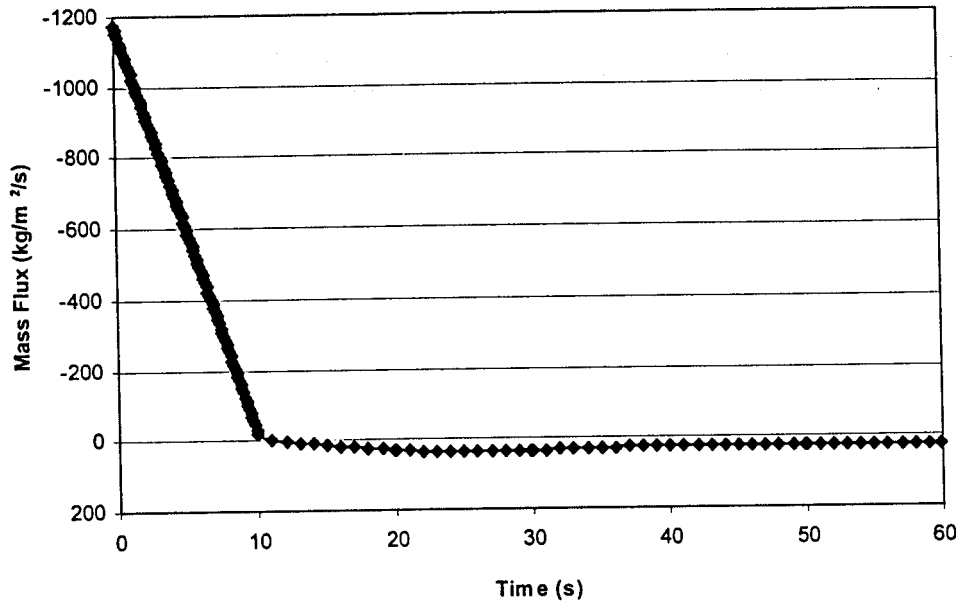


FIGURE 6.10: LINEAR MASS FLUX PROFILE

Temperatures vs. Time with Linear Flow Loss

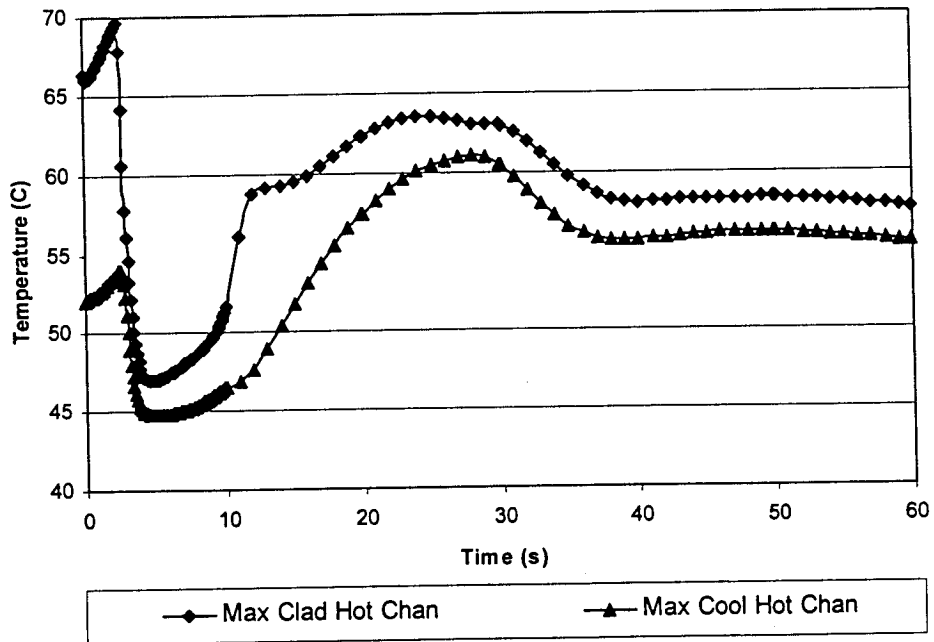


FIGURE 6.11: LINEAR TEMPERATURE PROFILE

Figure 6.12 shows the mass flux profile obtained from the loss-of-flow analysis for the exponential flow case. The flow reversal in this case occurs at approximately 45 seconds into the transient. Figure 6.13 shows the temperature profiles associated with the exponential case. The maximum cladding temperature in the hot channel was also approximately 70° C. However, this maximum actually occurs around the time of flow reversal, and is slightly higher than the initial maximum that occurs shortly after the reactor scram. Therefore, the exponential model is seen as the limiting case for the three loss-of-flow models.

Buoyancy forces exist which are associated with natural convection, due to the density differences between the coolant in the channel and the surrounding fluid. The pressure drop initially overwhelms these forces due to the decaying pump head. In all three models, the exit coolant temperatures drop shortly after the reactor scram due to a rapid decrease in power produced, and then rise sharply as the flow decreases. Higher buoyancy effects result from the reduced flow and increased coolant temperatures. Eventually, the buoyancy forces and the forces due to pump head are the same magnitude during the transient. At this point, a period of low flow occurs, and the net forces turn upward, which causes the flow inversion. As the flow reverses, the coolant that fails to escape the bottom of the reactor is heated further as it flows upward, causing the buoyancy forces and the natural convection mass flow rates to peak after the flow inversion. The peak clad temperature then quickly falls off after the hot slug of fluid is ejected from the top of the reactor core.

As a final comparison between the three flow loss models, the hot channel peak cladding temperature versus time is shown in Figure 6.14. This shows the exponential model as the limiting loss-of-flow case, due to the highest maximum cladding temperature, and the fact that it occurs during the flow inversion. However, the margin to ONB for the exponential case is greater than the instantaneous step-change reactivity model. Therefore, loss-of-flow is not seen as the limiting accident scenario in the transient analysis.

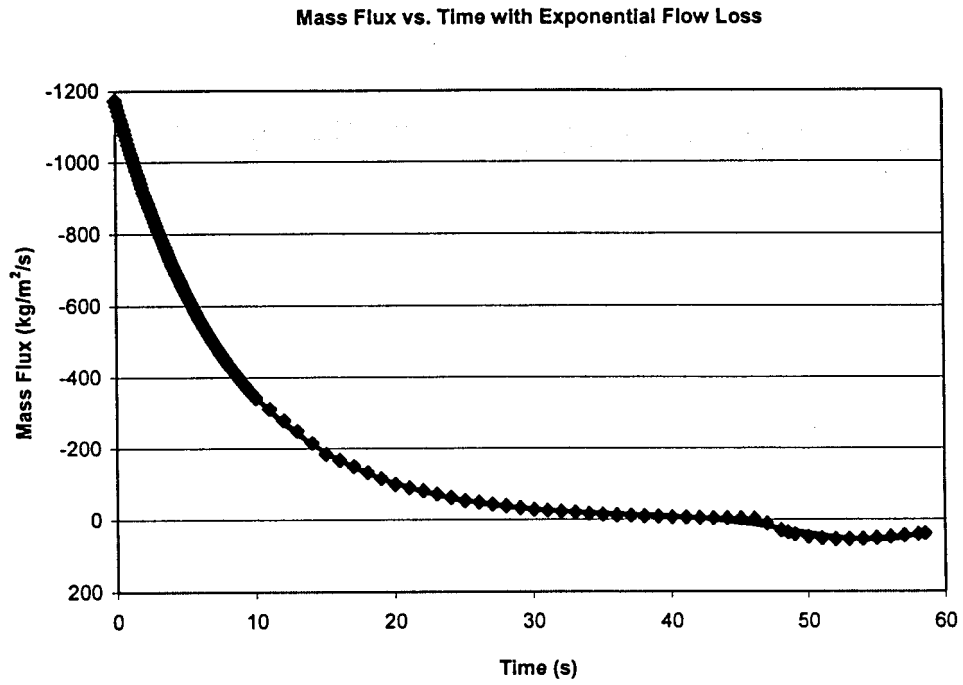


FIGURE 6.12: EXPONENTIAL MASS FLUX PROFILE

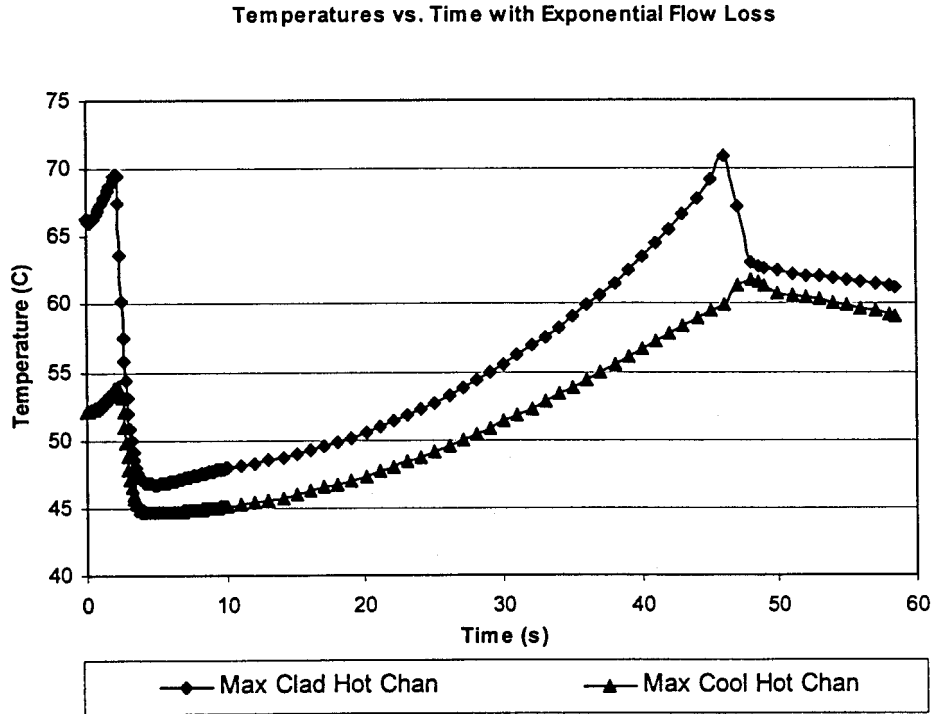


FIGURE 6.13: EXPONENTIAL TEMPERATURE PROFILE

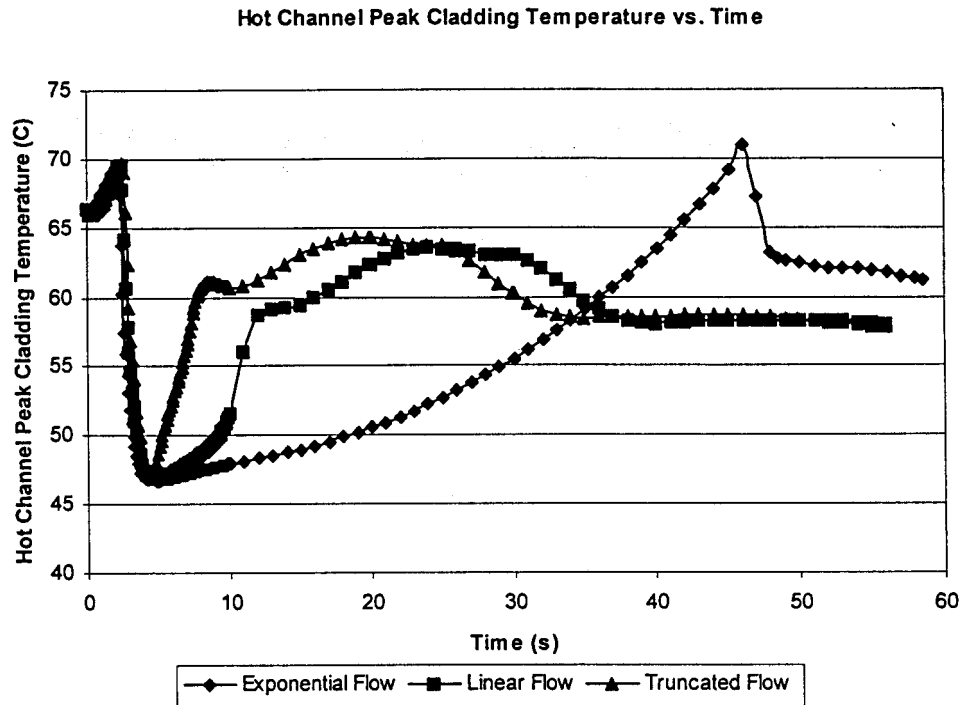


FIGURE 6.14: CLADDING TEMPERATURE COMPARISON FOR FLOW LOSS MODELS

6.3.4 PARET-ANL Power-to-Flow Map

From the above analyses, the instantaneous step-change reactivity transient was determined to be the limiting transient case. Therefore, it was necessary to determine what combinations of power and flow would cause the ONB to occur during a step-change reactivity transient. The reactivity worth of 0.5% $\Delta k/k$ was held constant, as it was determined to be the worst-case scenario of single failure criterion reactivity insertion. ONB for both forced- and natural-convection flow rates was established. This was done in a manner similar to that described for the PLTEMP analysis, where ONB was bracketed for a given power level between two very close flow rates. ONB was determined for forced-convection with power levels ranging from 100 kW to 6 MW, and for natural-convection from 100 kW to 600 kW. Under 600 kW, the ONB points for forced- and natural-convection were very close, with the forced-convection points requiring a slightly higher flow rate to prevent ONB. The flow direction (up or down flow) had very little effect on the ONB point, at least at low power levels. Therefore, only the forced-convection points were used in the development of the power-to-flow map.

The PARET-ANL power-to-flow map is shown in Figure 6.15. The curve represents the combination of power and flow that will cause ONB to occur at the maximum anticipated reactivity transient. As can be seen, the nominal forced-convection

operating condition of 2 MW and 2,000 gpm leaves a large margin to ONB even if the maximum reactivity transient occurs. PARET-ANL does not have the capability to model hot channel factors explicitly, so that uncertainty is not included in the PARET-ANL power-to-flow map shown in Figure 6.15. If that uncertainty were to be included, the new transient power-to-flow map would represent the best estimate of when ONB would occur, using conservative hot channel factors, for all foreseen accident conditions. The difference between the two PLTEMP steady-state power-to-flow curves shown in Figure 5.1 was used as a guide in determining what the uncertainty should be. The solution to the PARET-ANL hot channel factor modeling problem will be addressed in the next section.

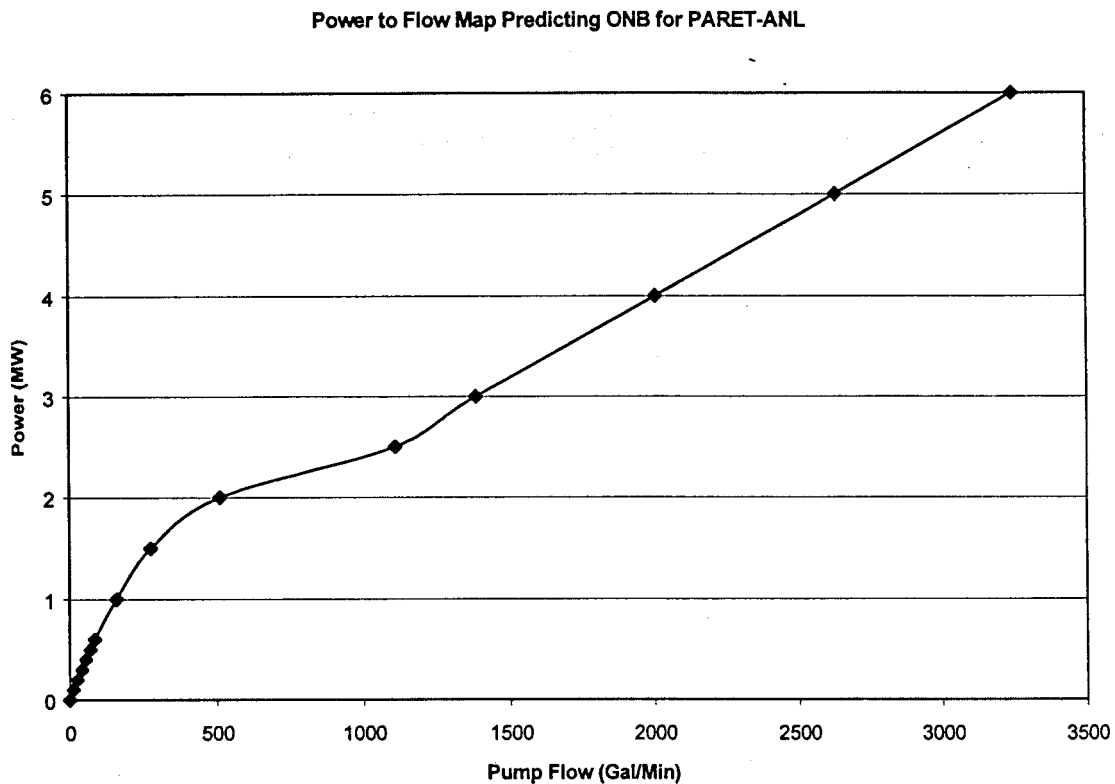


FIGURE 6.15: PARET-ANL POWER-TO-FLOW MAP

7.0 REACTOR ANALYSIS SUMMARY

The computer codes NATCON, PLTEMP, and PARET-ANL were used to determine the limiting conditions for safe operation of the current UMLRR LEU core under steady-state natural-convection, steady-state forced-convection, and transient conditions, respectively. These codes allow the user to set values for the power, flow rate, and in the case of PARET-ANL, reactivity transients, to determine what combinations of these parameters cause the onset of nucleate boiling (ONB) to occur. The ONB point is used as the single criterion for determining the safe operating conditions of the UMLRR. This limiting criterion, although very conservative, allows for safe operation of the UMLRR.

The NATCON steady-state convection thermal hydraulic computer code was used to determine the ONB point under natural-convection flow conditions. This occurred at a power level of 622 kW with a flow rate of 171 gpm. Hot channel factors were then incorporated in the model. Hot channel factors represent uncertainties in the flow rate, power level, and heat transfer coefficient. The particular uncertainties used in the current analysis included a flow uncertainty of about 25%, a heat flux uncertainty of 25%, and a heat transfer coefficient uncertainty of 35%. After the inclusion of hot channel factors, the ONB point was determined to occur at a power level of 392 kW with a flow rate of 126 gpm. At a power level of 200 kW, the natural-convection flow rate was determined to be 92 gpm without hot channel factors, and 87 gpm with hot channel factors.

The PLTEMP steady-state forced-convection thermal hydraulic computer code was used to create a power-to-flow map. The results of the power-to-flow map are used to define the steady-state operating envelope for the UMLRR. A given power level was put into the PLTEMP code, and by narrowing in on the pressure change, the flow rate just above and below where ONB occurs at the given power level can be determined. The flow rate just below ONB was then used to set the flow envelope criterion. By running this scenario at different power levels, a curve was generated for power-versus-flow rate, above which ONB will occur, assuming all the input parameters are known with a high degree of certainty. This sets the minimum pump flow rate for the UMLRR at a given power level to prevent ONB during steady-state operating conditions. This analysis was done for several power levels ranging from 600 kW to 6 MW. For a power level of 2 MW, ONB occurs somewhere between a flow rate of 702 to 707 gpm during steady-state conditions.

The same hot channel factors that were used in NATCON were then included in the PLTEMP input files. New flow rates bracketing ONB were determined, and another curve, which incorporates hot channel factors, was generated on the power-to-flow map. This provides the safety criterion used for steady-state operations. The margin between these two curves varies from approximately 60% at low power levels to approximately 75% at high power levels. These results are shown in Figure 7.1.

It should be noted that a similar steady-state power-to-flow map was used in the original safety analyses for the LEU core (for a slightly different configuration). This

map was used as the limiting condition of operation for both the steady-state and transient operating conditions of the system. This limiting condition was expected to be extremely conservative for transient situations because the peak power only occurs for very short time intervals (typically less than 1 second). However, since a transient power-to-flow map was not available, it was decided to simply use this very conservative methodology.

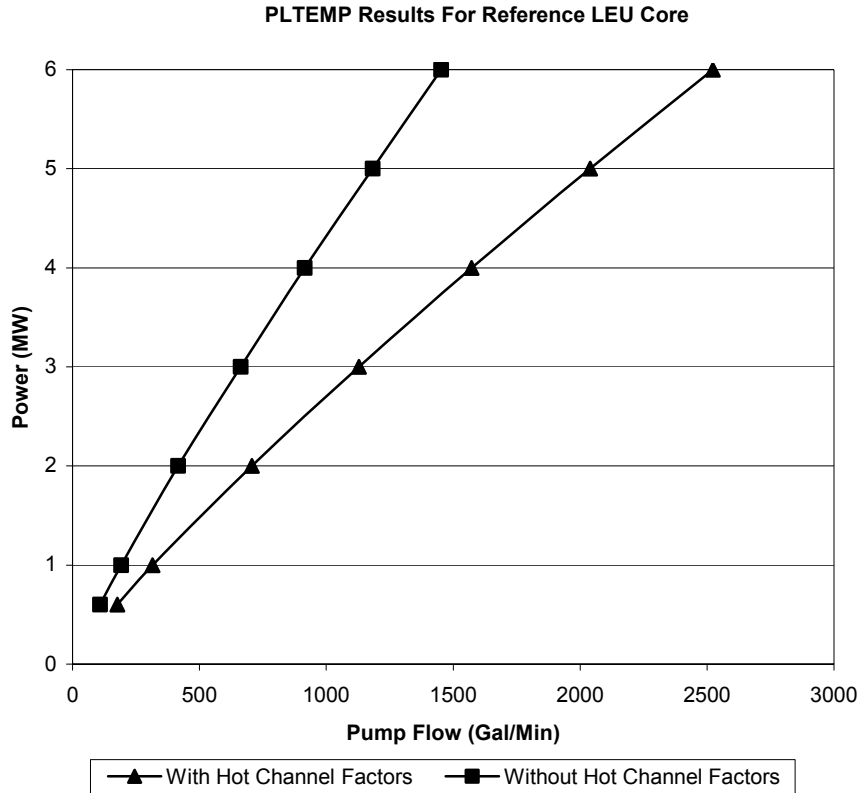


FIGURE 7.1: PLTEMP POWER-TO-FLOW MAP

To address this issue in the current study, the PARET-ANL transient thermal hydraulic computer code was used to determine the limiting conditions of operation for various reactivity transient and loss-of-flow scenarios. It was determined that the most limiting case was when an instantaneous, or step-change reactivity excursion of 0.5% $\Delta k/k$ (64 cents) occurred. This corresponds to the single-failure criterion of one fixed sample of maximum reactivity-worth instantaneously ejecting from the reactor core. From this base case, the limiting conditions of power and flow to prevent ONB from occurring during the transient were determined. These data were obtained using a procedure similar to the steady-state calculations, by bracketing the observed transient ONB point between two flow rates for a given initial power level. The flow rate just below ONB was then used to set the flow envelope criterion. By running this scenario at different power levels, a curve was generated for initial power-versus-flow rate, above which ONB will occur, assuming all the input parameters are known with a high degree of certainty. This sets the minimum pump flow rate for the UMLRR at a given initial power level to prevent ONB during transient operations. This analysis was done for several power levels ranging from 100 kW to 6 MW. At a power level of 2 MW, ONB

occurs somewhere between a flow rate of 505 and 510 gpm during the worst-case reactivity transient.

Unlike PLTEMP, the PARET-ANL code does not have the capacity to model hot channel factors explicitly in the input files. To simulate the effects of this, a 75% margin reflecting the highest deviation in the corresponding PLTEMP curves was graphed along with the normal PARET-ANL ONB curve. This is shown in Figure 7.2. This margin represents the best estimate of the combination of all hot channel factors as a worst-case scenario uncertainty. The nominal condition of operation is assumed to be a power level of 2 MW and a flow rate of 2,000 gpm. A similar natural convection low power-low flow region is shown in Figure 7.3. For this case, the nominal operating point is assumed to be 200 kW and approximately 90 gpm of flow through the core.

The power-to-flow map was expanded into two plots to highlight the two proposed nominal operating regimes for the UMLRR, i.e. natural-convection mode at low power (200 kW) and forced-convection mode at high power (2 MW). These plots show that, even with large uncertainties included, transient ONB will not occur with a 0.5% $\Delta k/k$ step-reactivity change during either natural- or forced-convection operation. This is due to the fact that the transient times are extremely short (much less than one second), which do not allow for significant heatup of the coolant. Also, due to the large Doppler broadening effect of the LEU core, the power tends to peak and subsequently decrease even before the scram occurs at the 2-MW power level. The transient ONB curve is proposed as the safety criterion for any operational transients to prevent ONB from occurring in the UMLRR LEU core.

As a final comparison, a plot of the steady-state and transient power-to-flow ONB curves, including the effects of hot channel factors, is shown in Figure 7.4. As expected, the transient case for a 0.5% $\Delta k/k$ step-reactivity change reduces the safe operating region of the power-to-flow map relative to the steady-state case. The lower curve, which represents the transient ONB hot channel factor power-to-flow map, gives the best estimate of when ONB would occur, using conservative hot channel factors, for all foreseen accident conditions. The use of the transient ONB condition was shown to give a conservative safety margin for the worst-case reactivity transient under both forced-flow and natural-convection conditions. Thus, the transient ONB results given here should be used to set the actual safe operating limits for the LEU-fueled UMLRR. In particular, it shows the UMLRR can be operated safely at 200 kW in natural-convection mode and 2 MW under forced-convection.

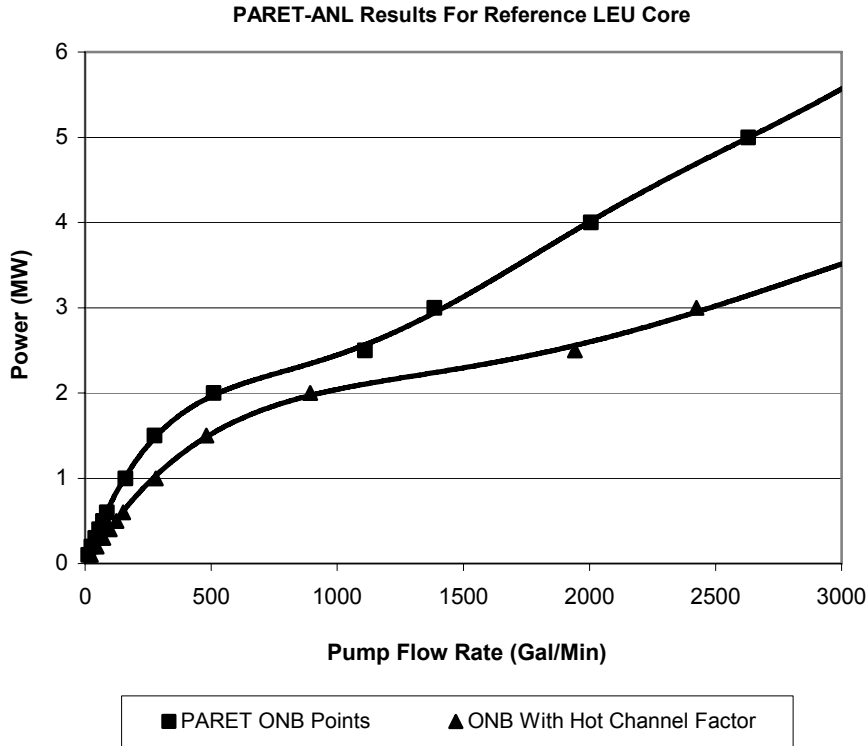


FIGURE 7.2: PARET-ANL HOT CHANNEL POWER-TO-FLOW MAP

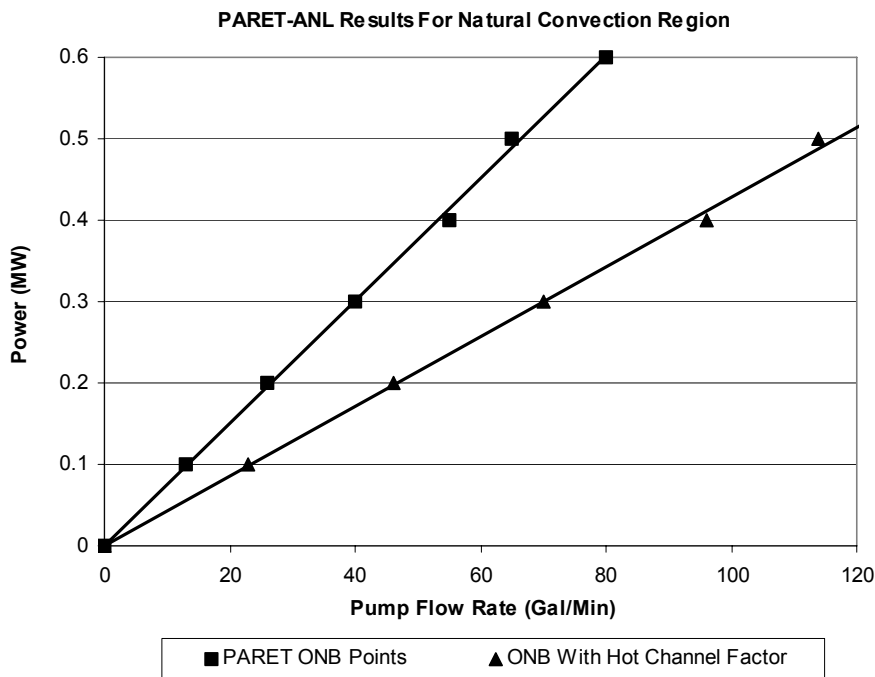


FIGURE 7.3: PARET-ANL NATURAL CONVECTION POWER-TO-FLOW MAP

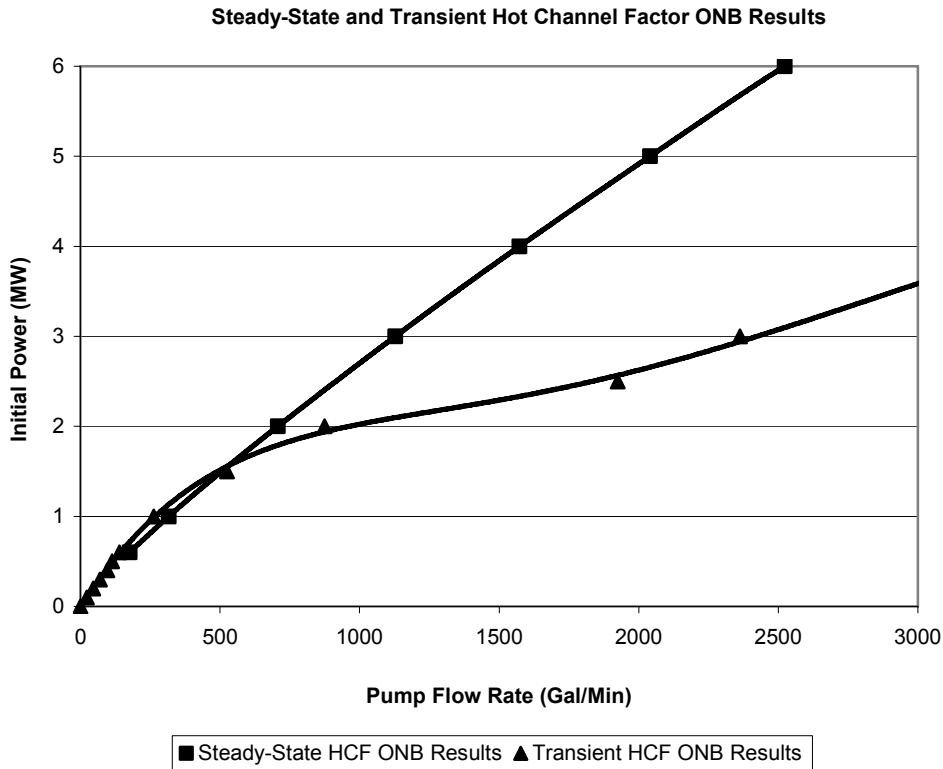


FIGURE 7.4: PLTEMP AND PARET-ANL HOT CHANNEL POWER-TO-FLOW MAPS

8.0 ADDITIONAL SAFETY ANALYSES

The UMLRR FSAR¹⁷ includes the analyses for a number of potential transients to verify that the safety limits are not exceeded. The effects of various postulated accidents also are analyzed. Of these, the NRC SER¹⁸ evaluates the maximum hypothetical accident in addition to three postulated events. In relation to an increased power level of 2 MW, the SER evaluated events are considered here.

8.1 REFUELING ACCIDENT

A refueling error is not an easy mistake because of the readily recognizable differences in fuel, graphite and reflector elements, because of the small core size and clearly recognizable reference points, and because any initial loading or subsequent loading or reloading is supervised during the process.

The most severe error imaginable is the substitution of a fueled element for the central flux trap element, and this has been calculated to add about 3% in reactivity.

Although such an error assumes considerable inattention by all loading personnel, nevertheless, if it occurred, the control blades have more than enough shutdown capability to assure that the reactor would be subcritical until some blade withdrawal was achieved. If such an error occurred, criticality would occur with the blades in a lower position than normal, which would cause the operator to shut the reactor down before going to power.

Dropping a fuel element on top of the core would add less than 0.5% in reactivity, and this, again is well within the shutdown capability of the blades.

8.2 STEP INCREASE IN REACTIVITY

Each experiment must be analyzed to assure that no more than 0.5% reactivity can be added under any condition.

An analysis of an instantaneous insertion of 0.5% reactivity at 2 MW power and 2,000 gpm flow was carried out by Stevens.⁴ The analysis is described in detail previously in this report. The result is shown in Figure 7.2. This margin represents the best estimate of the combination of all hot channel factors as a worst-case scenario uncertainty. The nominal condition of operation is assumed to be a power level of 2 MW and a flow rate of 2,000 gpm. A similar natural convection low power-low flow region is shown in Figure 7.3. For this case, the nominal operating point is assumed to be 200 kW and approximately 90 gpm of flow through the core.

8.3 LOSS OF COOLANT

A comprehensive loss of coolant analysis is provided in the FSAR for two cases. In one case, the core is partially uncovered (e.g., beam port rupture). The second case is for the highly unlikely complete loss of pool water wherein the core is completely uncovered. Both cases are analyzed for infinite operation above 2 MW. The case for partial core exposure concludes that for an infinite operation at 5 MW prior to the partial loss of coolant, the result is no clad failure. In the case for complete loss of pool water, an infinite operation at 3 MW does not result in clad failure.

9.0 STANDBY SAFEGUARDS ANALYSIS

9.1 ESTIMATION OF CONSEQUENCES OF FISSION PRODUCT RELEASE

The FSAR LEU Supplement contained an analysis of the release of fission products from a single fuel plate as the design accident which would have the greatest effect on offsite radiation releases. Though any postulated mechanism for this to occur is extremely remote, this accident scenario has been reevaluated in view of an increased power level to 2 MW.

The consequences of the release of gaseous fission products to the primary coolant and then to the containment space and then finally out of containment are presented below. The effect of additional plutonium in the LEU core was not considered in this analysis because of the analysis by Woodruff et. al.¹⁹ which showed that the additional plutonium in the LEU core had a minimal effect in the production of radioiodines and noble gas radioisotopes even with high burnups.

The scenario considered involves the release of all of the inert gases and radioiodides from a single fuel plate after 100 consecutive days of maximum power (2 MW) operation. The resulting thyroid and whole body dose equivalents were calculated at the exclusion boundary for conservative release and dispersion conditions. The exclusion boundary is 48 meters from the containment as explained in the FSAR.

9.1.1 Dose Calculations

The calculation of thyroid doses is based on the model and methodology used by Woodruff et. al.¹⁹ which takes into account activity losses within containment (plating out, etc.), diffusion after release from containment and decay losses. The thyroid dose equivalent (H_t) to an individual exposed to the release plume for a given time (t) is given by the following expression:

$$H_t = \text{sum}(H_i + H_s)$$

where H_i = internal dose equivalent

$$= \frac{X}{Q(t)} [Q_i(t) BR(t) DCF_i]$$

and $X/Q(t)$ = atmospheric diffusion factor in s/m^3
 $Q_i(t)$ = quantity of isotope released in millicuries
 $BR(t)$ = breathing rate of exposed individual during exposure
 DCF_i = dose conversion factor in rem per millicurie inhaled

and H_s = submersion dose equivalent

$$\frac{X}{Q(t)} [Q_i(t) BR(t) DCF_s]$$

and DCF_s = dose conversion factor in mrem per mCi/m^3 (submersion).

The atmospheric diffusion factor (X/Q) was determined assuming a ground level release during Pasquill type F conditions.

The quantity of each isotope released $Q_i(t)$ was determined according to the following formula:

$$Q_i(t) = F_R F_q q \frac{\lambda_i}{\lambda_i + \lambda_r} (1 - e^{-(\lambda_i + \lambda_r)t})$$

where: F_R = fraction of isotope released to containment
 F_q = fraction of isotope in containment released from containment
 q = inventory of isotope in a single fuel plate in millicuries
 λ_r = decay constant of isotope in hr^{-1}
 λ_l = leakage rate from containment in hr^{-1}
 t = time of exposure in hours.

The inventory of each of the iodine isotopes was derived from values published by Woodruff et. al.¹⁹ for the situation where the LEU fuel is irradiated at 1 MW for 100 continuous days. A peaking factor of two was applied to each quantity for these analyses. Quantities for each iodine isotope are listed in Table 9.1.

TABLE 9.1: QUANTITIES OF IODINE ISOTOPES RELEASED FROM A SINGLE FUEL PLATE

Isotope	Quantity Released (Curies)
I-131	164.4
I-132	250.9
I-133	394.9
I-134	444.2
I-135	369.0

Table 9.2 lists the quantities of inert gases that are assumed to be released from a single fuel plate into the containment.

TABLE 9.2: QUANTITIES OF INERT GASES RELEASED FROM A SINGLE FUEL PLATE

Isotope	Quantity Released (Curies)
Kr-83m	30.45
Kr-85m	75.23
Kr-85	0.32
Kr-87	145.57
Kr-88	205.87
Kr-89	267.80
Xe-131m	01.14
Xe-133m	11.56
Xe-133	392.00

Xe-135m	63.12
Xe-135	31.56
Xe-138	358.92

One hundred percent of the iodine activity and inert gas activity in a single plate is assumed to be released to the reactor pool during the postulated accident. All of the inert gas escapes into containment. Ten percent of the iodine is assumed to be released from the pool into containment (F_R).

Fifty percent of the iodines in containment is then assumed to be released outside of containment (F_Q). The leakage rate from containment is assumed to be ten percent per day. This is the designed leakage rate from containment with an overpressure of two inches of water.

The X/Q value used in this analysis was calculated using a regimen proposed in Regulatory Guide 1.145²⁰ where building effects and meandering plume effects are taken into account for Pasquill F conditions at low wind speed. The wind speed was assumed to be one meter per second. Changes in elevation or any other local conditions which might disperse the plume were not addressed. The value of X/Q used in this analysis was 0.031 sec/m³ at a horizontal distance of 48 meters from the containment structure.

The dose conversion factors were taken from the Health Physics and Radiological Health Handbook²¹ and USEPA's Federal Guidance Report No. 11.²²

9.1.2 Thyroid Doses

Thyroid doses at a distance of 48 meters from the containment building (site boundary) were calculated for a two-hour and an infinite-time release. These doses are presented in Table 9.3.

TABLE 9.3: THYROID DOSE EQUIVALENTS (REMS) AT FORTY EIGHT METERS FROM CONTAINMENT RELEASE POINT FOR GROUND LEVEL RELEASES

Type of Release	Iodine	Isotopes	Inert Gases	Total	Guideline
	External	Internal			
Two-Hour	0.0043	1.09	0.025	1.12	300
Infinite	0.0265	52.1	0.093	52.2	300

Greater than 98% of the thyroid doses come from the iodines deposited internally in the thyroid. Over 95% of the thyroid dose comes from I-131 and I-133.

9.1.3 Whole Body Dose Equivalents

Whole Body Dose Equivalents forty-eight meters from the containment release point were calculated for ground level releases and are given in Table 9.4.

TABLE 9.4: WHOLE BODY DOSE EQUIVALENTS (REMS) AT FORTY EIGHT METERS FROM CONTAINMENT RELEASE POINT FOR GROUND LEVEL RELEASES

Type of Release	Iodine	Isotopes	Inert Gases	Total	Guideline
	External	Internal			
Two-Hour	0.0036	0.033	0.0246	0.061	25
Infinite	0.0236	1.560	0.0864	1.673	25

The whole body dose equivalents are a result of a combination of effective dose from iodines in the thyroid (internal) and external exposure to the iodines and inert gases in the plume. The iodines were responsible for 61% of the two-hour release doses and 93% of the infinite-time releases.

CONCLUSION

The accidental release of radioiodines and inert gases from a single fuel plate under conditions resulting in a maximum inventory of these isotopes results in thyroid and whole body dose equivalents well below the two-hour site boundary guidelines from USNRC 10 CFR 100. In fact, the thyroid and whole body dose equivalents for infinite-time releases are also well below the guideline values.

REFERENCES

1. UML Staff, FSAR Supplement for the Conversion to Low Enrichment Uranium (LEU) Fuel for the University of Massachusetts Lowell (UML) Reactor, University of Massachusetts Lowell, May 1993.
2. J. R. White, J. Byard, and A. Jirapongmed, "Calculational Support for the Startup of the LEU-Fueled U Mass-Lowell Research Reactor," Topical Meeting on Advances in Reactor Physics and Mathematics and Computation, Pittsburg, PA, May 2000.
3. "Report on the HEU to LEU Conversion of the University of Massachusetts Lowell Research Reactor," submitted to the US Nuclear Regulatory Commission in fulfillment of Amendment No. 12 to License No. R-125 (April 2001).
4. A. Stevens, "Thermal Hydraulic Analyses of the University of Massachusetts Lowell Research Reactor," M.S. Thesis, University of Massachusetts Lowell (Dec 2000).
5. R. S. Smith, W. L. Woodruff, "NATCON, Steady State Thermal Hydraulics Code for Natural Convection in Research Reactors," RERTR Program, Argonne National Laboratory, July 1987.
6. K. Mishima, K. Kanda, T. Shibata, "Thermal Hydraulic Analysis for Core Conversion to the Use of Low Enriched Uranium Fuels in the KUR," Research Reactor Institute, Kyoto University, Japan, December 1984.
7. C. F. Obenchain, "PARET, A Program for the Analysis of Reactor Transients," Phillips Petroleum Company, AEC Research and Development Report, January 1969.
8. W. L. Woodruff, "A Users Guide for the Current ANL Version of the PARET Code," RERTR Program, Argonne National Laboratory, 1999.
9. J. P. Phelps, et al., "Final Safety Analysis Report for the Lowell Technological Institute Reactor," University of Lowell, September 1973.
10. J. Byard, "Informational Retrieval System for the Life of the LEU-Fueled U Mass-Lowell Research Reactor," M. S. Thesis, Energy Engineering, University of Massachusetts Lowell, June 2001.
11. J. R. White, et al., "Design and Initial Testing of an Ex-Core Fast Neutron Irradiator for the U Mass-Lowell Research Reactor," Radiation Protection and Shielding Topical Conference, Santa Fe, New Mexico, April 2002.
12. UML Staff, Proposed Technical Specifications for the University of Massachusetts Lowell Reactor with Low Enrichment Fuel, University of Massachusetts Lowell, February, 1994.

13. Code of Federal Regulations, Title 10 (Energy), Part 20.1302 (2) (ii), page 295.
14. A. Amarnath, "Thermal Hydraulic Analysis of the HEU and the Proposed LEU Core Configurations of the U Mass Lowell Research Reactor," M. S. Thesis, Energy Engineering, University of Massachusetts Lowell, 1993.
15. R. S. Freeman, "Neutronics Analysis for the Conversion of the ULR from High Enriched Uranium to Low Enriched Uranium Fuel," M. S. Thesis, Energy Engineering, University of Massachusetts Lowell, 1991.
16. W. L. Woodruff, "The PARET Code and the Analysis of the SPERT I Transients," RERTR Program, Argonne National Laboratory, 1982.
17. Final Safety Analysis Report for the University of Lowell Research Reactor, License No. R-125, Docket No. 50-223, Submitted February 1985.
18. NUREG-1139 Safety Evaluation Report Related to the Renewal of the Operating License for the Training and Research Reactor at the University of Lowell, Docket No. 50-233, November 1985.
19. W. L. Woodruff, D. K. Warinner, J. F. Matos, "A Radiological Consequence Analysis with HEU and LEU Fuels," IAEA TECDOC-643, 1992.
20. USNRC Regulatory Guide 1.145, "Atmospheric Dispersion Models for Potential Accident Consequence Assessments at Nuclear Power Plants," 1982.
21. "The Health Physics and Radiological Handbook," Edited by B. Scleien, Scinta Inc., 1992.
22. Federal Guidance Report No. 11, "Limiting Values of Radionuclide Intake and Air Concentration Dose Conversion Factors for Inhalation Submersion and Ingestion," ORNL and USEPA, 1988.